New room temperature nematogens by cyano tail termination of alkoxy and alkylcyanobiphenyls and their anchoring behavior on metal salt-decorated surface

Kunlun Wang[a], Tibor Szilvási[b], Jake Gold[b], Huaizhe Yu[c], Nanqi Bao[c], Prabin Rai[a], Manos Mavrikakis[b], Nicholas L. Abbott[c], and Robert J. Twieg[a*]

[a]Department of Chemistry and Biochemistry,

Kent State University, Kent, OH 44242 USA

[b]Department of Chemical and Biological Engineering,

University of Wisconsin-Madison, Madison, WI 53706 USA

[c] Department of Chemical and Biomolecular Engineering, Cornell

University, Ithaca, NY14853 USA

* Author for Correspondence: rtwieg@kent.edu

Abstract

A series of cyano tail-terminated alkoxy and alkyl cyanobiphenyl compounds and some cyano-p-terphenyl derivatives were synthesized and mesogenic properties described. Comparison with the K series and M series indicates that the terminal cyano group generally enhances the supercooling of the molecules. Furthermore, several binary LC mixtures formed by the cyano tail-terminated compounds were found exhibiting promising room temperature nematic phases ranges comparable to the commercial quaternary mixture E7. The equimolar binary mixture of CN5OCB and CN7OCB shows homeotropic ordering at the metal salts-decorated surfaces and planar ordering at the free surface, which is consistent with G_{BE} values we calculated. As such, these materials are promising candidates for sensor devices which display a rapid response to a variety of analytes.

1. Introduction

The K series 4-alkyl-4'-cyanobiphenyl (nCB) and the M series 4-alkoxy-4'-cyanobiphenyl (nOCB) mesogens have found wide applications in the field of liquid crystal (LC) science [1]. The best-known compound in this series is undoubtably 4-*n*-pentyl-4'-cyanobiphenyl (5CB) due to its convenient room temperature nematic phase. The polar cyano group not only contributes to the stable nematic LC phases and opto-electronic properties [2,3] but is also utilized as a binding ligand on metal salts for chemoresponsive sensors [4,5]. In order to achieve enhanced mesogenic properties the pursuit of structural modifications of these cyanobiphenyl mesogens has never stopped. In addition to substitution on the aromatic rings [6–9] functionalization on the flexible tails, including terminal functionalization, also influences the phase behavior of LC molecules [10–15] (Figure 1). The polar hydroxy terminus generally increases the phase transition temperatures due to hydrogen bonding [13]. Studies indicate that the addition of a halogen atom (chlorine or bromine) to the terminus of the tail strongly promotes the formation of a smectic A phase in related difluoroterphenyl [10] and phenylpyrimidine [11] systems. In contrast, the halogen terminus is also reported to slightly decrease the phase transition temperatures and clearing points and furthermore destabilize a smectic phase in cyanobiphenyl systems [12, 14].

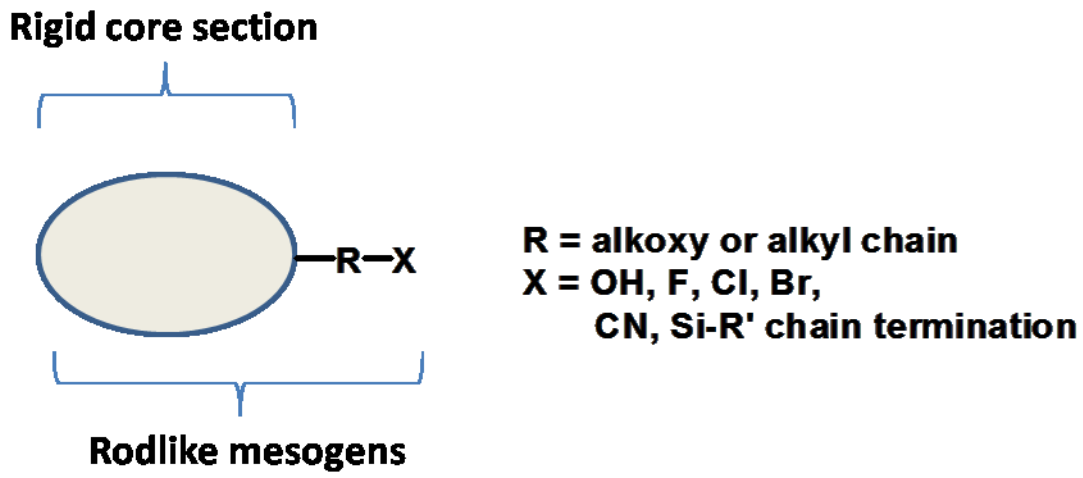

Figure 1. Some previously examined liquid crystal tail termini functionalization.

The cyano group often plays a key role as a polar end group when attached to a central rigid core. Previously, some mesogens with cyano terminated alkoxy tails have been reported — tolane derivatives by P. Adomenas et al [16]; stilbene derivatives by Y.Y. Daugrila et al. [17]; benzoates and azobenzenes based molecules by E. I. Rjumtsev et al. [18] and B. I. Ostrovskii et al. [19] respectively; and also biphenyl based [20] and benzylidene [21] based compounds by F. Barbarin et al. However, to our knowledge, the influence of the cyano tail termination on the mesogenic properties of the cyanobiphenyl system has not yet been systematically studied.

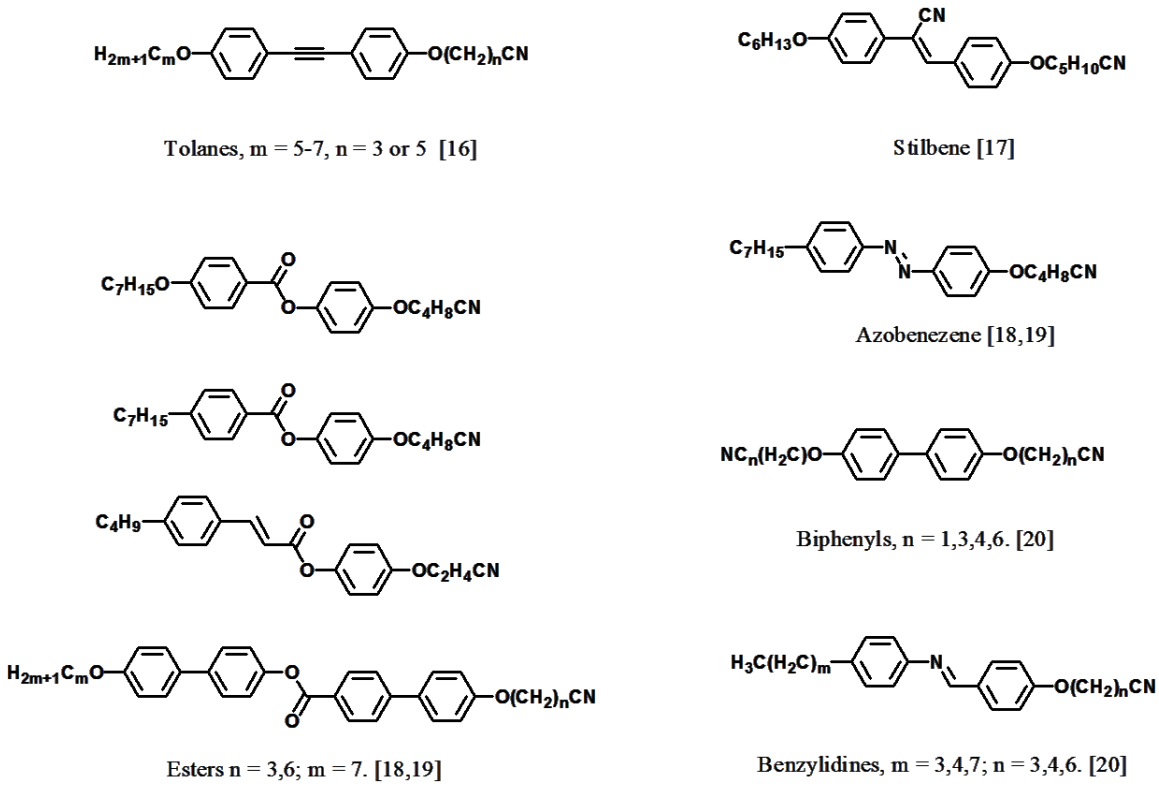

Figure 2. Some previously examined cyano tail terminated LCs.

Based on our previous experience with terminal tail functionalization [13,14], a series of cyano tail terminated alkoxy/alkyl cyanobiphenyl compounds have been synthesized. Most important, new liquid crystal mixtures based on these terminal tail-functionalized molecules have been identified that exhibit a wide nematic phase including room temperature. Such broad ambient temperature nematics are being pursued due to their utility in many applications including our own pursuit of chemoresponsive sensors [4,5]. In such sensors we have found that CN4OCB, CN5OCB, and the mixture of CN5OCB and CN7OCB in 50%:50% molar ratio adopt homeotropic (perpendicular) ordering on surfaces supported with $Ni(ClO_4)_2$ metal salts, which is consistent with the negative G_{BE} values we calculated. Moreover, the nitrile terminated chain perturbs the smetic layer of molecules and gives rise to planar anchoring at the air interface. These

materials are promising candidates for sensor devices which display a rapid response to a variety of analytes.

2. Experimental Section

Commercial-grade solvents were used without further purification. $PdCl_2$ was purchased from Pressure Chemical (Pittsburgh, PA). Palladium on carbon (5%), diisopropylamine, ether and copper iodide were purchased from Acros. The precursor 4'-cyano-4-iodobiphenyl was prepared using a literature method [22]. The 4"-hydroxy-1,1':4',1"-terphenyl-4-carbonitrile was prepared by Suzuki coupling reaction of 1-bromo-4-hydroxybiphenyl and 4-cyanophenylboronic acid [23]. Triphenylphosphine and ethylenediamine were purchased from Sigma-Aldrich. The 4-bromobutyronitrile and 6-bromohexanenitrile were purchased from Alfa Aesar (Ward Hill, MA). The 5-bromovaleronitrile and 7-bromoheptanenitrile were purchased from Matrix Scientific (Columbia, SC). The hexafluorobenzene was purchased from Oakwood Products (Columbia, SC). Sodium cyanide was purchased from Mallinckrodt Chemical Works (New York, NY). The terminal hydroxyacetylenes were purchased from GFS Organic Chemicals (Columbus, OH). The compressed hydrogen was bought from Linde Gas. The products were purified by column chromatography using silica gel (60–120 mesh) and/or by recrystallization from analytical grade solvents.

Polarized optical microscopy (POM): Nikon ECLIPSE E600 Microscope & SPOT^{TM} idea COMS and Mettler Toledo FP90 central processor with FP82HT hot stage.

IR analysis was accomplished by using a Bruker Vector 33 FTIR spectrometer (Bruker Optics Inc, Billerica, MA, USA). The data obtained was processed and plotted using OPUS software (ver. 6.5, Bruker Optics Inc, Billerica, MA, USA).

A Bruker 400 NMR was used for NMR data acquisition (Frequency: 400 MHz for 1H-NMR; 100 MHz for ^{13}C-NMR and 376 MHz for ^{19}F-NMR) and the plots were generated by TOPSPIN 2 software (ver. 2.1, Bruker Optics Inc., Billerica, MA, USA).

A Thermo Finnigan Trace - GC 2000 (Thermo Scientific, Austin, TX, USA) and Polaris Q Mass Spectrometer (Thermo Scientific, Austin, TX, USA) were used to follow the reactions and assay product purity. The GC-MS data was collected and processed via Xcalibur software (Ver. 1.4, Thermo Scientific, San Jose, CA, USA).

Differential scanning calorimetry (DSC) analysis was run on a 2920 Modulated DSC from TA instruments (TA Instruments Inc., New Castle, DE, USA). Experimental data was analyzed and exported by using the Thermal Advantage software (Version 1.1A, TA Instruments Inc., New Castle, DE, USA).

General Procedure for the synthesis of cyano tail-terminated alkoxy cyanobiphenyl/ terphenyl compounds (reaction between phenol and α,ω-bromoalkanenitrile)

In a 200 ml round bottom flask was placed 4-cyano-4'-hydroxybiphenyl (1.0 equiv.), an α,ω-bromoalkanenitrile (1.0 equiv.), dry DMF (1.0 mL for each 1.0 mmol substrate), potassium carbonate (2.0 equiv.) and potassium iodide (0.1 equiv.). The resulting suspension was stirred overnight at room temperature and the reaction was monitored by TLC analysis. Once complete, water was added dropwise with stirring to fill the flask and the precipitate was collected by vacuum filtration. In some cases when no precipitate was found, the mixture was extracted with dichloromethane. The crude product was recrystallized from methanol. (yields from 56%-88%)

This geneneral procedure was utilized for cyano terminated CNnOCB (n = 3-6) and CNnOCT (n = 3-6) as well as the chloro terminated compound Cl5OCB. The cyano terminated CN2OCB was synthesized using a different method (see SI).

General Procedure for the synthesis of 4'-ω-tosylalkoxy/alkyl-4-cyanobiphenyl compounds (reaction between terminal alkanol and *p*-toluenesulfonyl chloride)

The reactions were carried out according to a literature method [13]. A 100 ml flask was charged with the 4'-ω-hydroxyalkoxy/alkyl-4-cyanobiphenyls (2.0-5.0 mmol), triethylamine (1.3 equiv.) and DCM (5.0-10.0 mL). The mixture was cooled to a temperature between 5°C-15°C and a solution of *p*-toluenesulfonyl chloride (1.0 equiv.) in DCM (5.0-10.0 mL) was added slowly via an additional funnel. Once the addition was complete, the reaction mixture was warmed to ambient and stirred for 12 hours. The reaction was monitored by TLC until completion and was terminated by addition of silica gel and the mixture was concentrated to dryness. The product was purified by column chromatography eluted with hexanes and ethyl acetate (4:1) to afford the desired tosylate derivative. (yields from 67%-76%)

Representative procedure for the cyanation (synthesis of CN7OCB from the relevant tosylate)

To a solution of 4'-[[7-[[(4-methylphenyl)sulfonyl]heptyl]oxyl]-4-cyanobiphenyl (1.1 g, 3.0 mmol) in DMSO (15 mL) was added NaCN (186 mg, 3.8 mmol). The mixture was stirred for 8 hours at 60 °C and after this time TLC indicated the reaction was complete. The residue was dissolved in water (30 mL) and extracted from the aqueous phase with diethyl ether (15 mL). The organic phase was dried over magnesium sulfate and

evaporated under reduced pressure. The desired product CN7OCB was purified by column chromatography eluted by ethyl acetate:hexane (1:4) as white crystals, which was then recrystallized from methanol as a white solid. (Yield: 440 mg, 46%)

This route was utilized for CN7OCB and CNnCB (n = 5-7).

For detailed procedures, see the supplementary information.

Computational methods

All calculations were carried out using Gaussian 09 version D.01 [24]. Density functional theory (DFT) at the PBE-D3(SMD=benzonitrile)/def2-SVP level of theory [25-28] was used for all geometry optimizations. Subsequently, dipole moments were calculated for each obtained structure at the M06-2X-D3(SMD=benzonitrile)/def2-TZVP level of theory [29]. Several conformers, especially local minima, play a role in determining the overall dipole moment of compounds. To obtain an appropriate statistical sampling of the conformational modes of the aliphatic chains of mesogens, the complete conformational space was generated by assuming three stable conformations (one anti and two gauches) for each C-C and C-O single bonds of the aliphatic chain. Therefore, the assumed starting dihedral angle was 0, 120, or 240 degree for all single bonds investigated in the conformer search. To limit computational cost, the number of randomly chosen conformers were limited to 2000 conformers for each compound. These conformers were then used in the dipole moment calculations. To obtain the average dipole moment for each compound, the Boltzmann weighted sum of the dipole moment was calculated including all relevant conformers. This approach has been successfully benchmarked

against higher level computational methods [4] and has been used to accurately model mesogen properties including their dipole moments [13, 14].

To model the binding of mesogens to metal salts, we performed Binding Free Energy (G_{BE}) calculations at the M06-2X-D3/def2-TZVP//PBE-D3/def2-SVP level of theory using the Neutral Anion Model (NAM) which has been shown to provide good agreement with experiments, as described in detail previously [5, 30, 31]. G_{BE} of mesogens are calculated as $G_{BE} = G_{Model+LC} - G_{Model} - G_{LC}$, where $G_{Model+LC}$ is the total free energy of the metal salt cluster with the bound mesogen, G_{Model} is the free energy of the naked metal salt cluster and G_{LC} is the free energy of the mesogen molecule in the gas phase. Negative values of G_{BE} (i.e., binding) were found to correlate with homeotropic ordering of mesogens whereas positive G_{BE} indicated planar ordering. For the sake of simplicity and consistency, we investigated only the energetically most stable anti conformation of the aliphatic chain of the mesogens to calculate and compare G_{BE}.

3. Synthesis

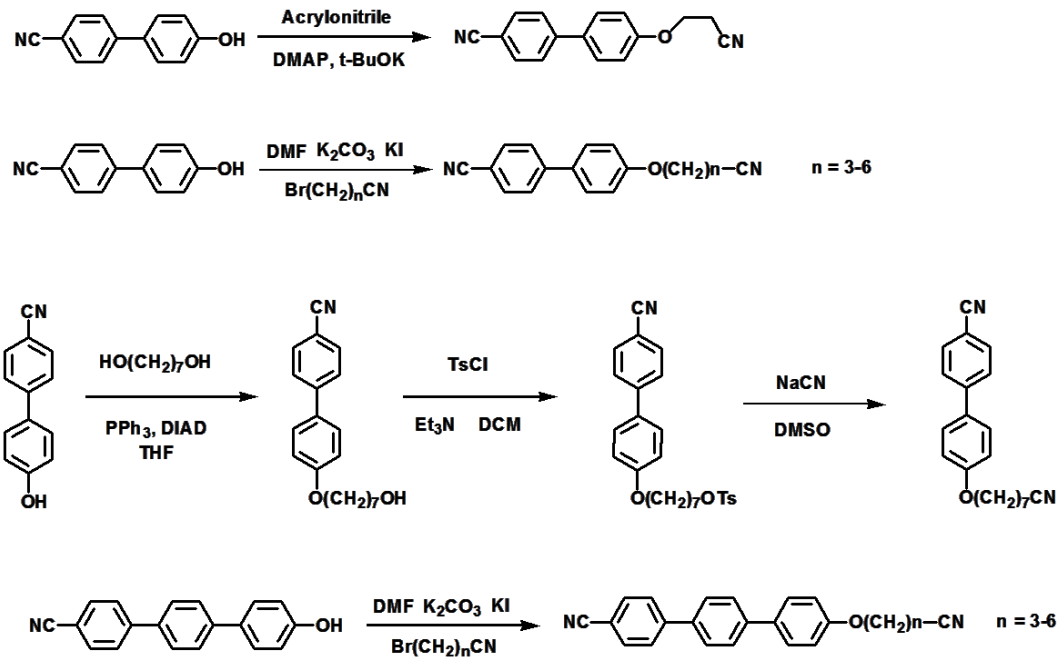

Scheme 1. The synthesis of cyano tail terminated alkoxy cyanobiphenyls CNnOCB and alkoxy cyanoterphenyls CNnOCT. The CN2OCB was synthesized from acrylonitrile while the CNnOCB (n = 3-6) and CNnOCT (n = 3-6) were synthesized from α,ω-bromoalkanenitriles. The CN7OCB was synthesized from the relevant hydroxy tail terminated cyanobiphenyl.

Different methods were chosen for synthesis of members of the same series based on the availability of relevant starting materials. Most of the cyano tail-terminated alkoxy cyanobiphenyl (CNnOCB) and cyanoterphenyl compounds (CNnOCT) were synthesized by standard alkylation of 4'-hydroxy-4-cyanobiphenyl or 4"-hydroxy-4-cyanoterphenyl with commercial α,ω-bromoalkanenitriles (n = 3-6 for CB series and n = 3-6 for CT series, Scheme 1). The one exception is CN2OCB, which was synthesized from acrylonitrile and 4'-hydroxy-4-cyanobiphenyl. The reactions proceed smoothly at room temperature and when complete, the product can be precipitated by the addition of water and collected by vacuum filtration. For the seven-carbon chain derivative a method used to synthesize fluorine terminated liquid crystals was utilized since the required bromoalkanenitrile with n=7 is not available [14]. The hydroxyheptyloxy cyanobiphenyl with a hydroxy group on the tail terminus was first prepared by a standard Mitsunobu reaction between the commercial precursors 4’-hydroxy-4-cyanobiphenyl and excess 1,7-heptanediol (Scheme 1). Next, the terminal alcohol was tosylated with *p*-TsCl in the presence of triethylamine in good yield. The cyanation was then accomplished using sodium cyanide in DMSO to give the desired cyano tail terminated heptyloxycyanobiphenyl. All the cyano terminated biphenyl compounds were recrystallized from methanol and the analogous terphenyl compounds from acetonitrile for characterization and thermal behavior study.

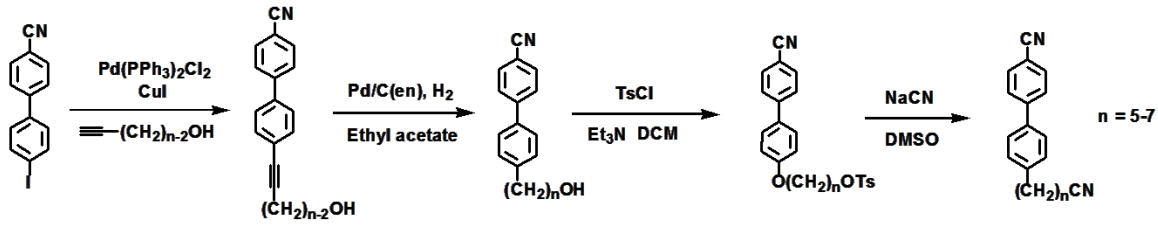

Scheme 2. The synthesis of cyano tail terminated alkyl cyanobiphenyls CNnCB.

The corresponding alkyl cyanobiphenyl derivatives were then pursued using the strategy described in our previous work on hydroxy terminated tails [13, 14, 32]. The hydroxy tail terminated alkyl cyanobiphenyls were first prepared and then tosylated in good yields (Scheme 2). The resulting tosylates were reacted with sodium cyanide under previously described conditions to yield the desired cyano tail terminated alkyl cyanobiphenyls (CNnCB).

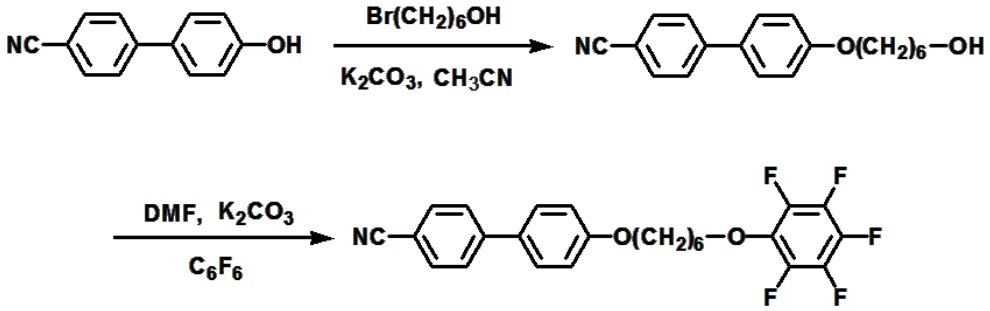

Scheme 3. The synthesis of pentafluorophenyloxy terminated hexyloxy cyanobiphenyl PF6OCB.

The compound 1-(4-cyanobiphenyl-4'-yloxy)-6-(pentafluorophenyloxy)hexane (PF6OCB) first reported by T. Itahara et al was utilized here in our studies to make broad temperature range nematic mixtures [33]. We used a different synthetic approach to make this substance than was previously reported. From our earlier work [13], 4'-[(6-hydroxy)hexyloxy-]4-cyanobiphenyl had been prepared as an intermediate (Scheme 3). This compound was treated with an excess of hexafluorobenzene in the presence of potassium carbonate in a polar aprotic solvent. The desired product resulting from a

single aromatic nucleophilic substitution was obtained in good yield without the formation of any byproducts.

4. Results and Discussions

The phase behavior of all the cyano tail terminated CB compounds were determined and are compared to the parent M series in Table 1. Similar to the M series (terminated with a methyl group), the cyano terminated CBs generally exhibit a nematic phase but with slightly narrower ranges. When n is 3 or 4 (CN3OCB and CN4OCB), they show monotropic behavior, which is consistent with their M series counterparts. Both CN5OCB and CN7OCB show enantiotropic behavior and thus the 50%:50% molar ratio binary mixture of these two compounds was investigated and a wide nematic range was obtained (-40 to 74.6 $^{\circ}$C in Figure 4). As CN4OCB shows supercooling nematic behavior, it was mixed with CN5OCB in a 50%:50% molar ratio and the resulting binary mixture also exhibits a wide nematic phase (< -40 to 71°C in Figure 5). Note that the nematic behavior of these two component mixtiures is comparable to the commercial nematic quaternary mixture E7 (-63 to 60 $^{\circ}$C) (Merck KGaA, Darmstadt, Germany). The CN2OCB and CN6OCB do not possess any intrinsic mesogenic properties. In terms of the temperature ranges, CN7OCB possesses a lower clearing point than the non-cyano terminated version. The other cyano tail terminated CBs all show higher clearing points. The DSC plot of CB5OCB is shown in Figure 4 and this mesogen exhibits significant supercooling, which may be a very useful behavior for the creation of LC mixtures.

	Phase behavior (°C)	
n	CNnOCB	M series
2	K 186 I 168 K	K 102 (N 91) I
3	K 138 I 79 N 71 K	K 72 (N 64) I
4	K 93 I 61 N 38 K	K 78 (N 76) I
5	K 66 N 77 I 76 N 4.9 K	K 50 N 68 I
6	K 97 I 68 K	K 57 N 76 I
7	K 61 N 71 I 71 N 15 K	K 54 N 74 I

Table 1. The phase behavior of the cyano tail terminated alkoxy CB compounds CNnOCB (K = Crystal, N = Nematic, I = Isotropic). Data available for the analogous parent non-substituted alkoxy M series is provided for comparison [34].

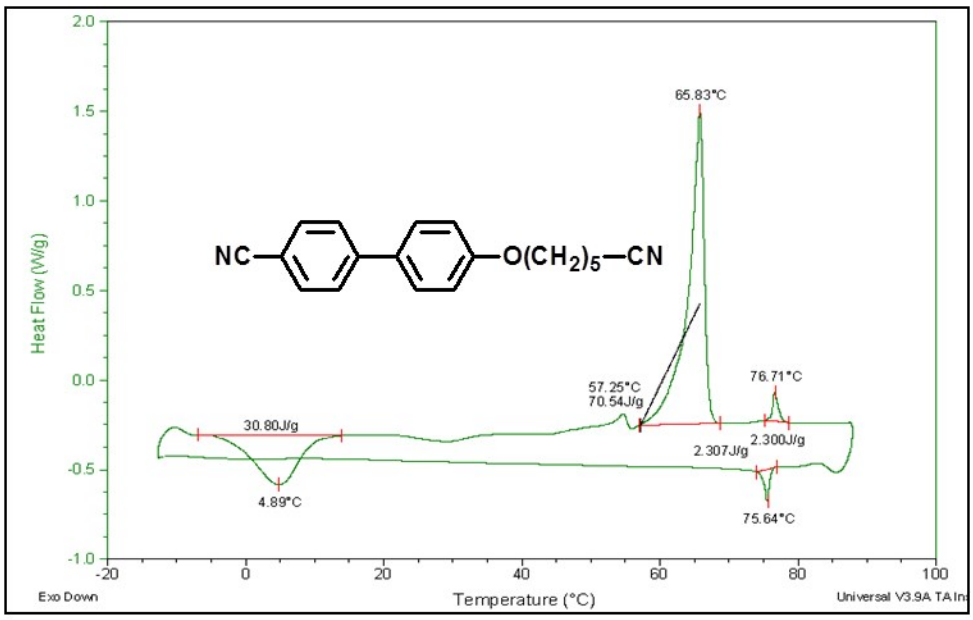

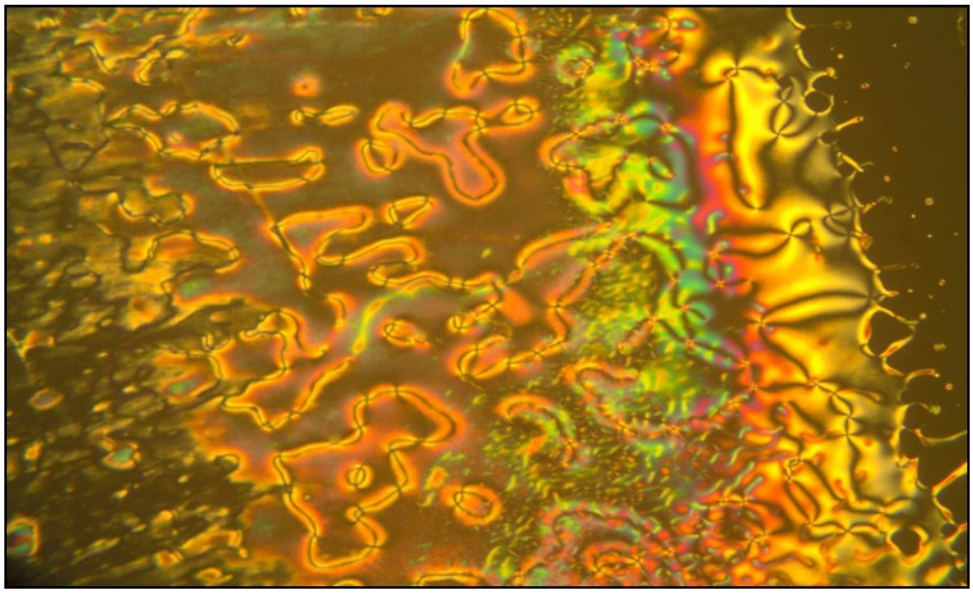

Figure 3. The DSC plot of pure CN5OCB (K 65.8 N 76.7 I) (top) and optical microscopy image (crossed-polars) of the nematic phase texture at 77 °C during transition from nematic to isotropic phase (bottom). Note the dramatic supercooling of the nematic phase of this substance.

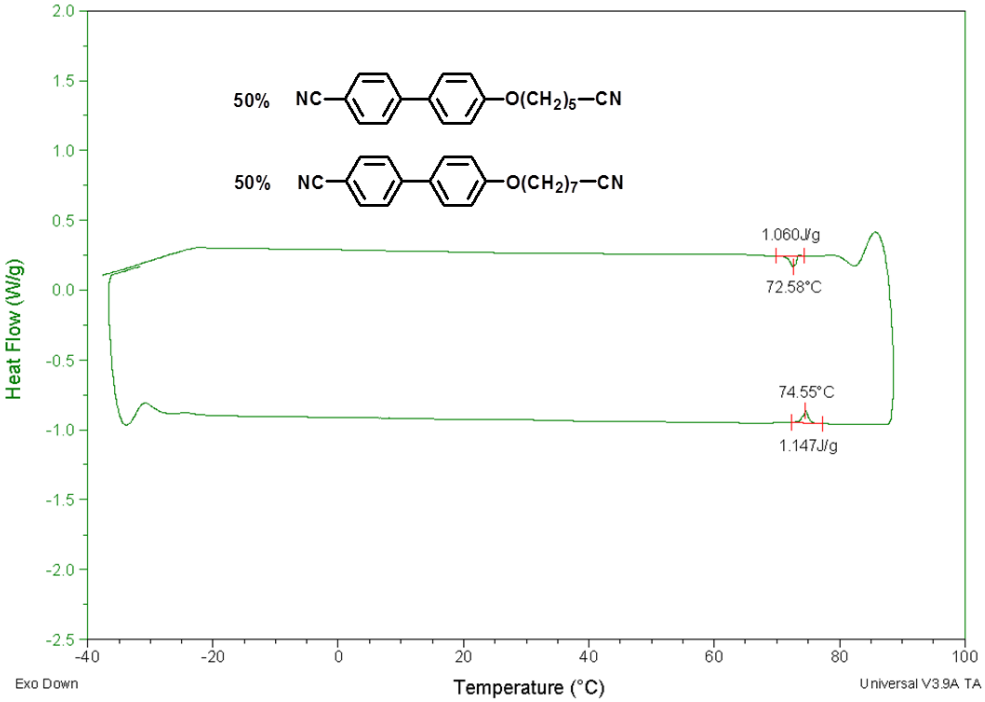

Figure 4. The DSC plot of the mixture of CN5OCB and CN7OCB in 50%:50% molar ratio (N 74.6 I 72.6 N). (The lowest cooling temperature was only down to -40 °C due to the limitations of the DSC).

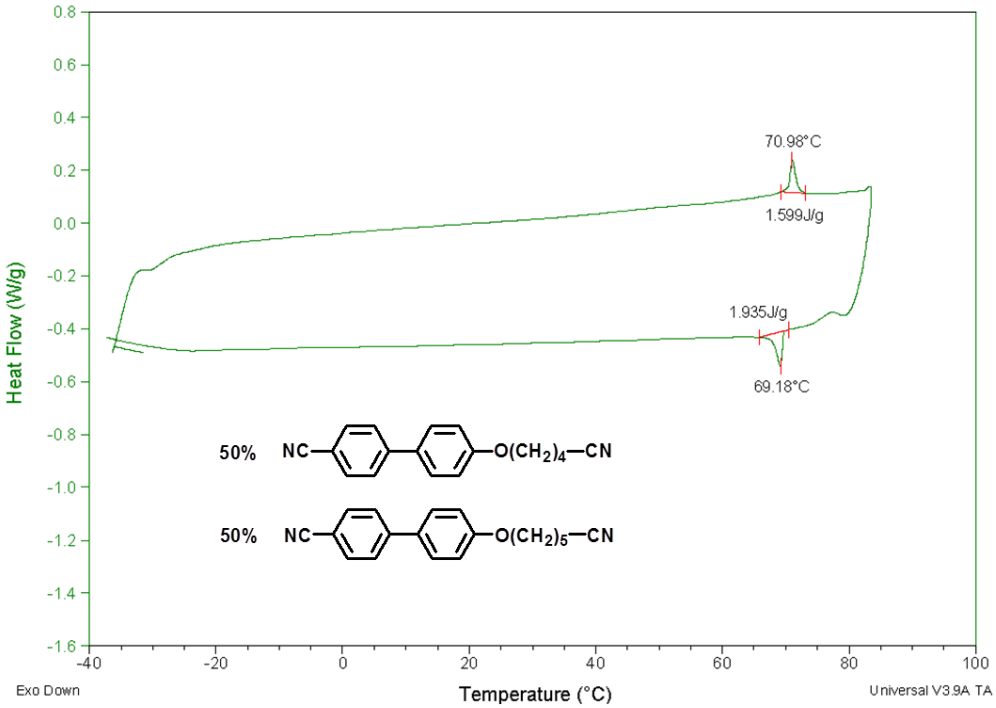

Figure 5. The DSC plot of the mixture of CN4OCB and CN5OCB in 50%:50% molar ratio (N 71.0 I 69.2 N). (The lowest cooling temperature was only down to -40 °C due to the limitations of the DSC).

Next, four cyano tail terminated alkoxy cyanoterphenyl compounds (CNnOCT) were examined (Table 2). The CN3OCT and CN4OCT generally show a wider nematic range than the parent non-terminal-functionalized cyanoterphenyls—lower crystal to nematic transition temperatures (T_{KN}) and higher clearing points (T_{NI}). The CN5OCT and CN6OCT have similar nematic ranges compared to the parent terphenyl compounds. The parent cyanoterphenyls all show a variety of smectic phases below the nematic phase but no smectic phases are observed for the two shorter cyano terminated derivatives CN3OCT and CN4OCT (Figure 6). This destabilization of smectic phase by terminal functionalization is consistent with previous results with halogen termination [12,14]..

	Thermal behavior (°C)	
n	CNnOCTs	OCTs
3	K 172 N 287 I 286 N 162 K	K 190 SmB 207 N 282 I Decomposed during DSC
4	K 141 N 271 I 271 N 134 K	K 121 Sm 185 N 272 I Decomposed during DSC
5	K 154 Sm 177 N 264 I 263 N 172 Sm 145 K	K 104 SmF 130 SmB 172 N 253 I
6	K 133 Sm 160 N 248 I 247 N 154 Sm 105 K	K 90 SmF 115 SmB 169 N 240 I

Table 2. The phase behavior of the cyano tail terminated alkoxy CT compounds CNnOCT (K = Crystal, N = Nematic, Sm = Smectic, I = Isotropic). Data available for the analogous parent nonsubsitituted alkoxy series is provided for comparison [35][1].

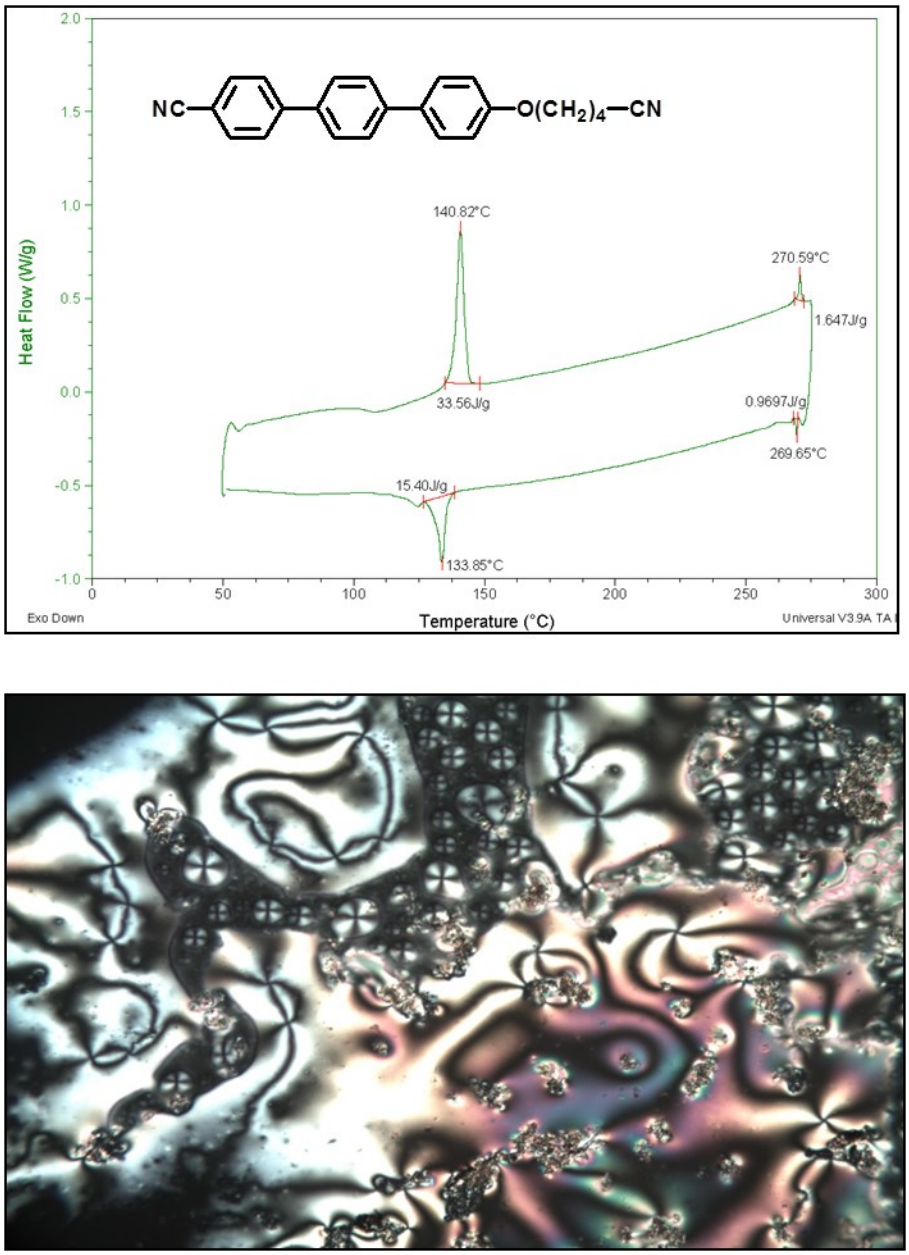

Figure 6. The DSC plot of pure CN4OCT (K 140.8 N 270.6 I) (top) and optical microscopy image (crossed-polars) of nematic phase texture at 266 ˚C (bottom).

The situation with the K-series cyanobiphenyl derivatives (CNnCB, currently only CN5CB, CN6CB and CN7CB have been obtained, Table 3) is different from the M-series cyanobiphenyl derivatives. The analogue CN4CB has been described in the

literature and prepared using a different method but its phase behavior is not reported [36]. The clearing points of these CNnCB cyano tail terminated compounds increase by approximately 20–30 °C compared to the parent K series but are 5–30 °C lower than the alkoxy analogous in Table 1. The CN6CB exhibits only monotropic nematic behavior whereas the other two compounds CN5CB and CN7CB possess no mesogenic properties. Similar to its alkoxy analogue, CN6CB also shows some supercooling according to the DSC (Figure 7).

	Phase behavior (°C)	
n	CNnCB	K series
5	K 68 I 25 K	K 22.5 N 35 I
6	K 61 I 35 N -7 K	K 15 N 30 I
7	K 66 I 36 K	K 31 N 44 I

Table 3. The phase behavior of the cyano tail terminated alkyl cyanobiphenyl compounds CNnCB (K = Crystal, N = Nematic, I = Isotropic) which have been prepared. Data available for the analogous parent nonsubsitituted alkyl series is provided for comparison [37].

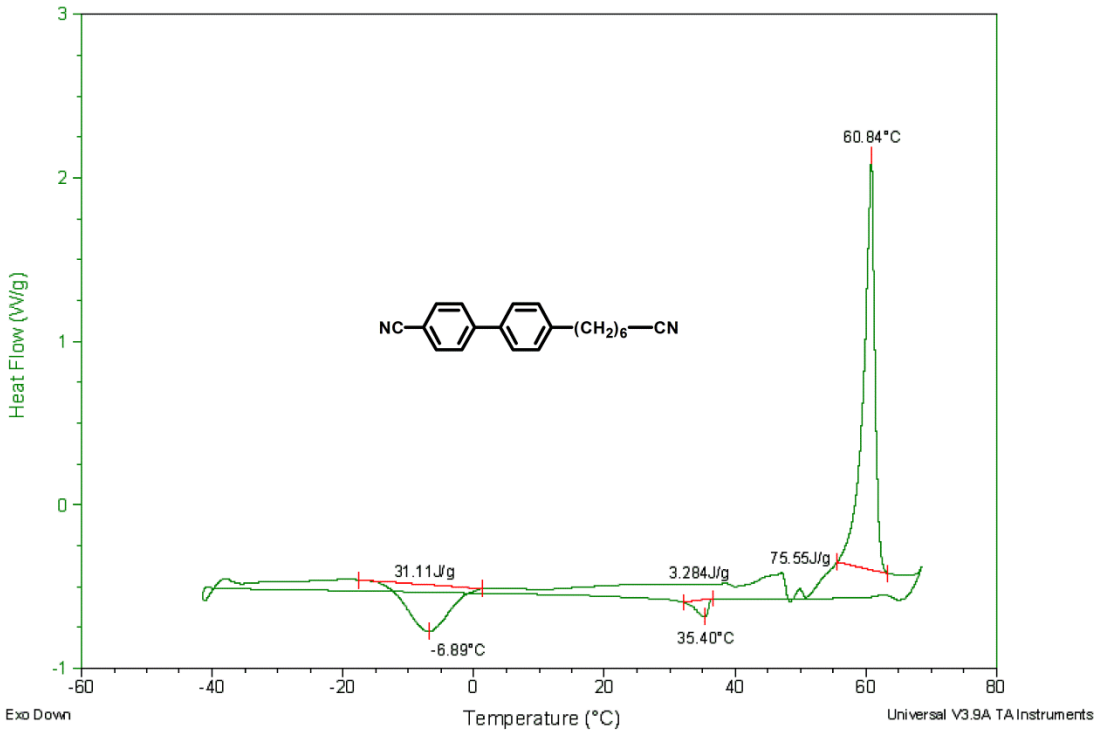

Figure 7. The DSC plot of CN6CB (K 60.8 I 35.4 N -6.9 I) showing the monotropic nematic phase and supercooling.

The terminal tail functionalization with a cyano group does not have an dramatic influence on the thermal behavior of the cyanobiphenyl system, especially for the alkyl analogues. However, according to our previous results [14] and the two cyano tail terminated CB mixtures described above, mesogens showing supercooling are very useful components to achieve a sub ambient nematic range. Here, the new molecule CN5OCB and a known chlorine tail terminated CB compound Cl5OCB [12] were selected for further study of liquid crystal mixtures. In addition, another terminal functionalized compound has attracted our attention: 4-(6-pentafluorophenyloxyhexyoxy)-4'-cyanobiphenyl (PF6OCB). This compound was originally synthesized by T. Itahara to study even/odd effect of different spacers [33].

Within the PFnOCB series Itahara reports that PF6OCB has a low T_{KN} and the widest nematic range. Interestingly, our DSC analysis also shows that PF6OCB has very strong supercooling properties (Figure 8). The pure compound shows nematic state at ambient conditions and then eventually crystallizes after a couple of days. A mixture made from M21 (7OCB) and PF6OCB in equal molar ratio was investigated and a near-ambient nematic phase (27–67 °C) was obtained accompanied by supercooling as shown in Figure 9. This sample crystallizes in the next heat cycle according to DSC and stays nematic at ambient conditions for weeks. The reason why M21 was selected is because M21 also supercools significantly by itself. Hence, the combination of two supercooling mesogens may give rise to some interesting outcomes.

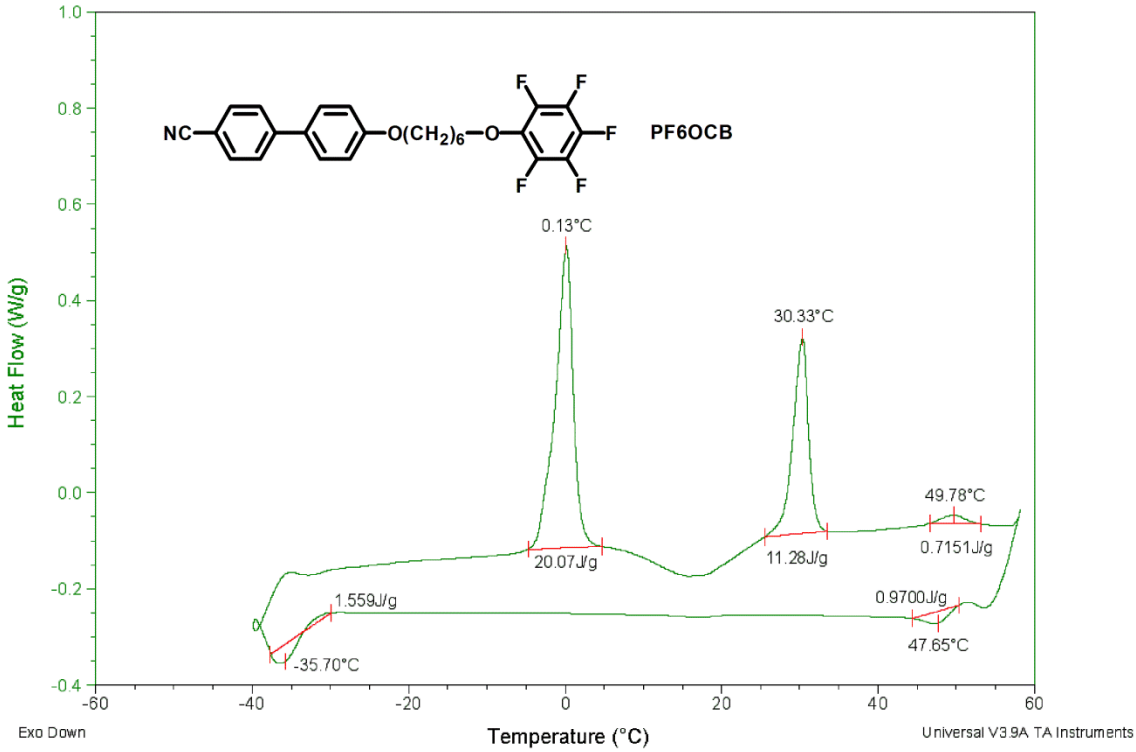

Figure 8. The DSC plot of pure (K_1 0.1 K_2 30.3 N 49.8 I 47.7 N -35.7 K). Note the significant nematic supercooling in this sample. (The lowest cooling temperature was only down to -40 °C due to the limitations of the DSC).

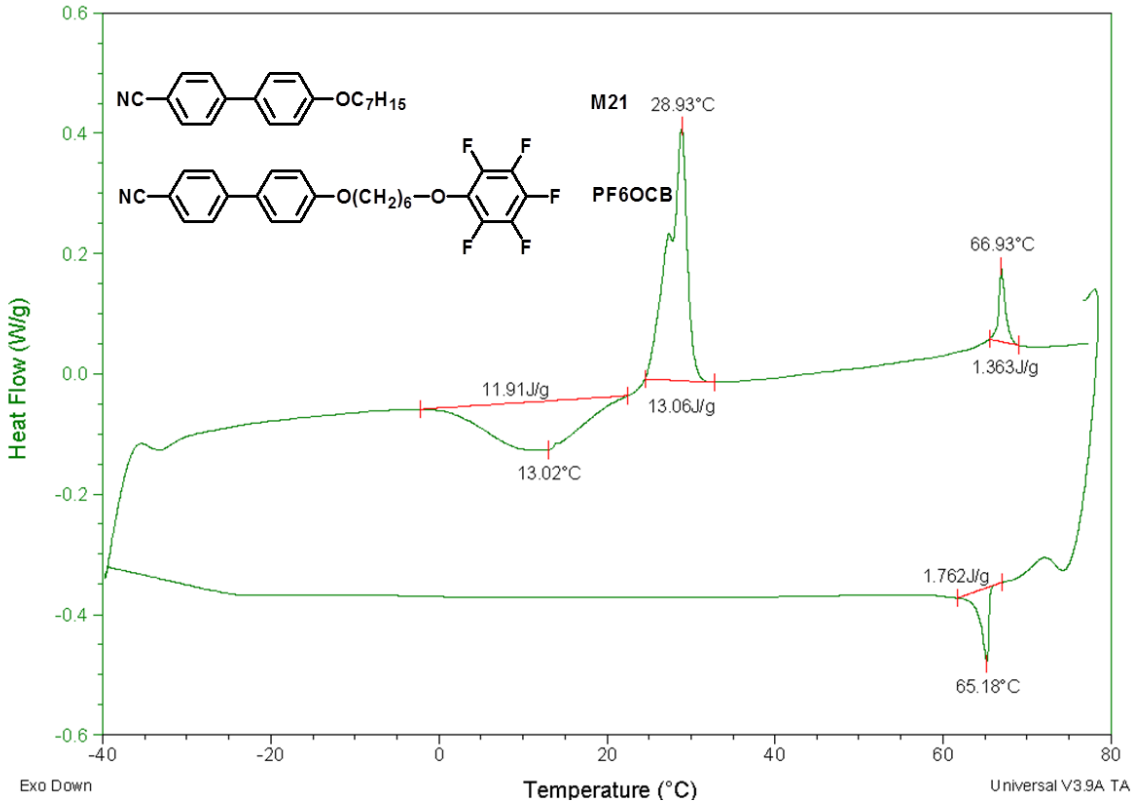

Figure 9. The DSC plot of the 50%:50% mixture of M21 and PF6OCB (K 28.9 N 66.9 I 65.2 N 13.0 K in the next cycle). (The lowest cooling temperature was only down to -40 °C due to the limitations of the DSC).

The examination of binary mixtures of PF6OCB and CN5OCB in different ratios is shown in Figure 9. The clearing points of all the binary mixtures vary little (from 60 to 73 °C) over the entire composition range. When the molar percentage of PF6OCB ranges from 20% to 90% the resulting mixtures possesses a remarkably broad nematic phase down to -40 °C (the plateau is an artifact due to the low temperature limitation of the DSC) (Figure 10). For example, the 50%:50% mixture exhibits a nematic phase from -40 to 64.4 °C (Figure 11). This may derive from the higher clearing point of CN5OCB as well as the supercooling properties of both components. The mixture of PF6OCB (20%) and CN5OCB (80%) also shows this supercooling property during the cooling cycle but

the transition of nematic to isotropic appears quite broad. Thus, this ratio has been chosen as the minimum amount requirement of PF6OCB. These samples stay in a liquid crystal state for weeks under ambient conditions.

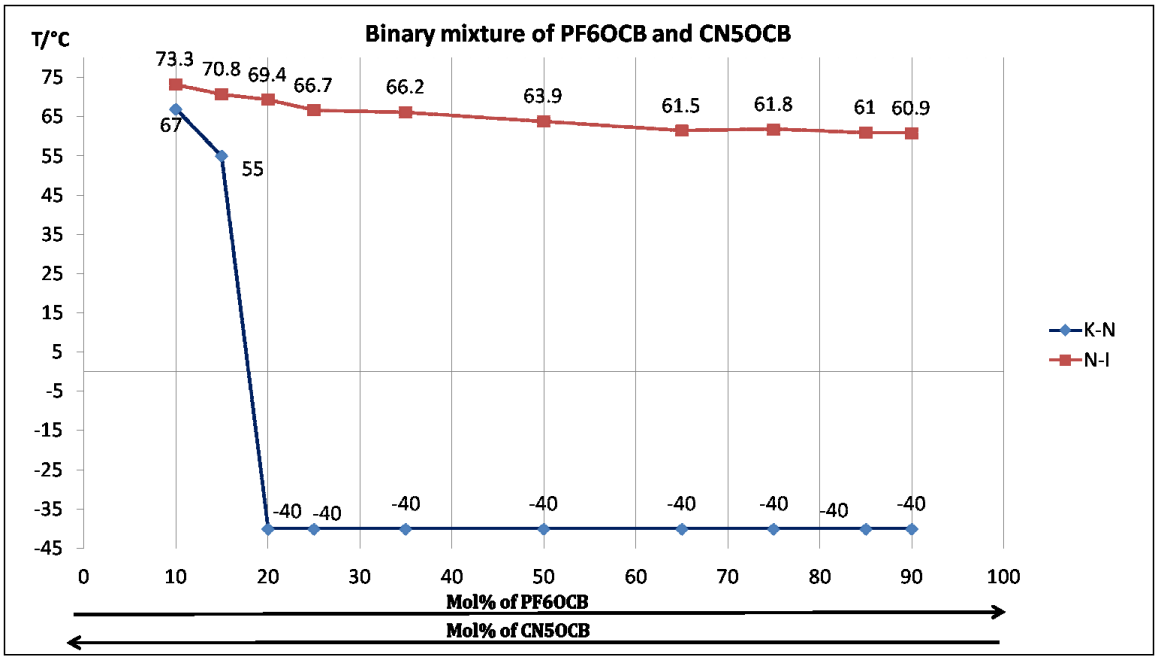

Figure 10. The phase behavior data of the binary mixtures of PF6OCB and CN5OCB. The temperature plateau at -40 °C is an artifact due to the limitation of the DSC.

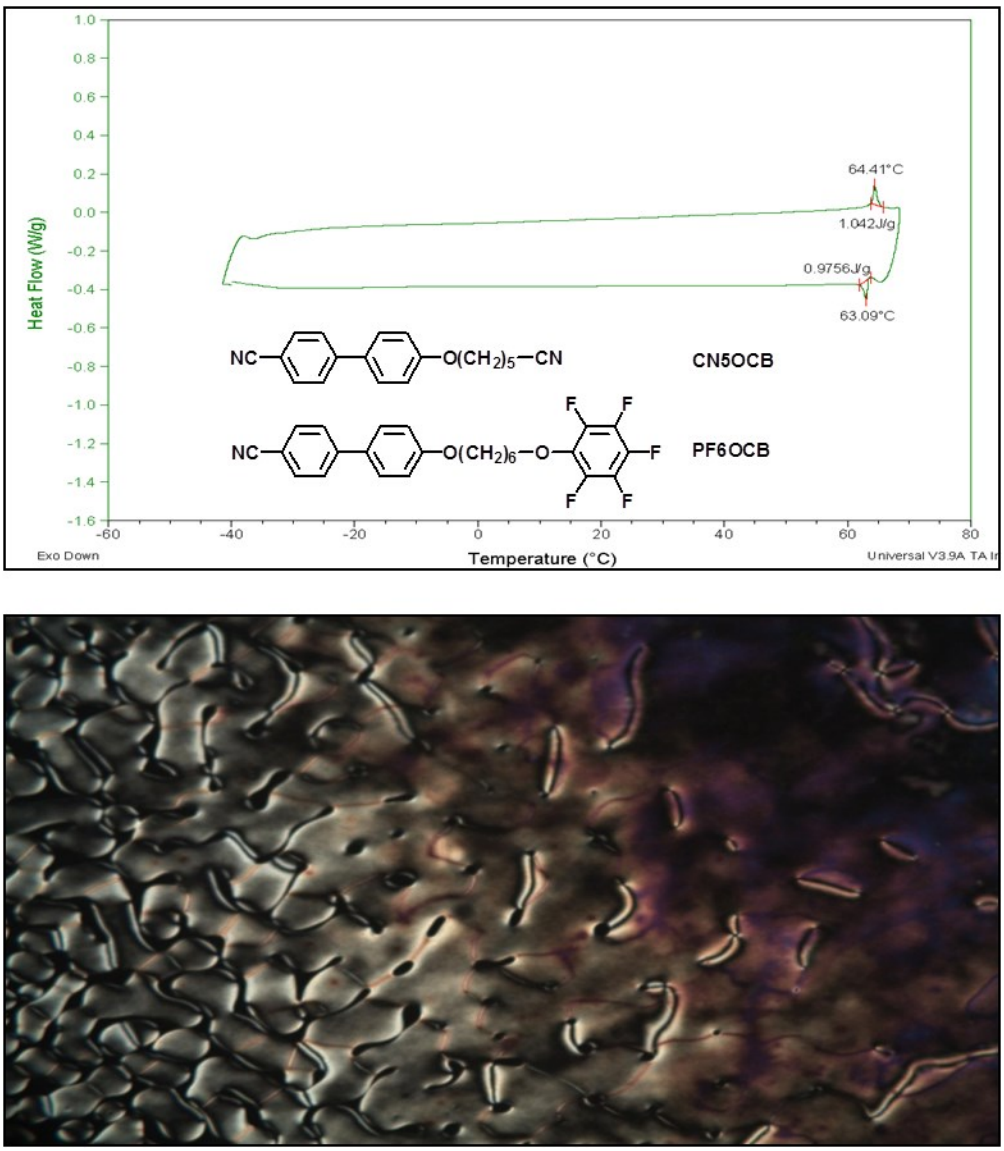

Figure 11. The DSC plot of the mixture of PF6OCB and CN5OCB in 50%:50% molar ratio (N 64.4 I) (top) and optical microscopy image (crossed-polars) of nematic phase texture at 64 °C the transition from nematic to isotropic phase (bottom). (The lowest cooling temperature was only down to -40 °C due to the limitations of the DSC).

The thermal behavior of the binary mixtures of PF6OCB and Cl5OCB in different ratios is shown in Figure 11. The clearing points ranges from 60 to 65 °C. When the

molar percentage of PF6OCB ranges from 40% to 75% the resulting mixtures possesses a broad nematic phase down to -40 °C (the plateau is an artifact due to the low temperature limitation of the DSC) (Figure 12). This ratio range is not as wide as the mixture of PF6OCB and CN5OCB but still it provides a range of room temperature nematic compositions. In particular, the 50%:50% mixture exhibits a nematic phase from -40 to 58.1 °C (Figure 13). It is interesting to see the monotropic behavior of Cl5OCB did not have a negative influence on the phase behavior of the resulting mixture. When the molar percentage of PF6OCB is below 40% or above 75%, the mixtures crystallize easily during cooling and no longer appear nematic state at near room temperature. Otherwise, the mixtures also stay in a liquid crystal state for weeks under ambient conditions.

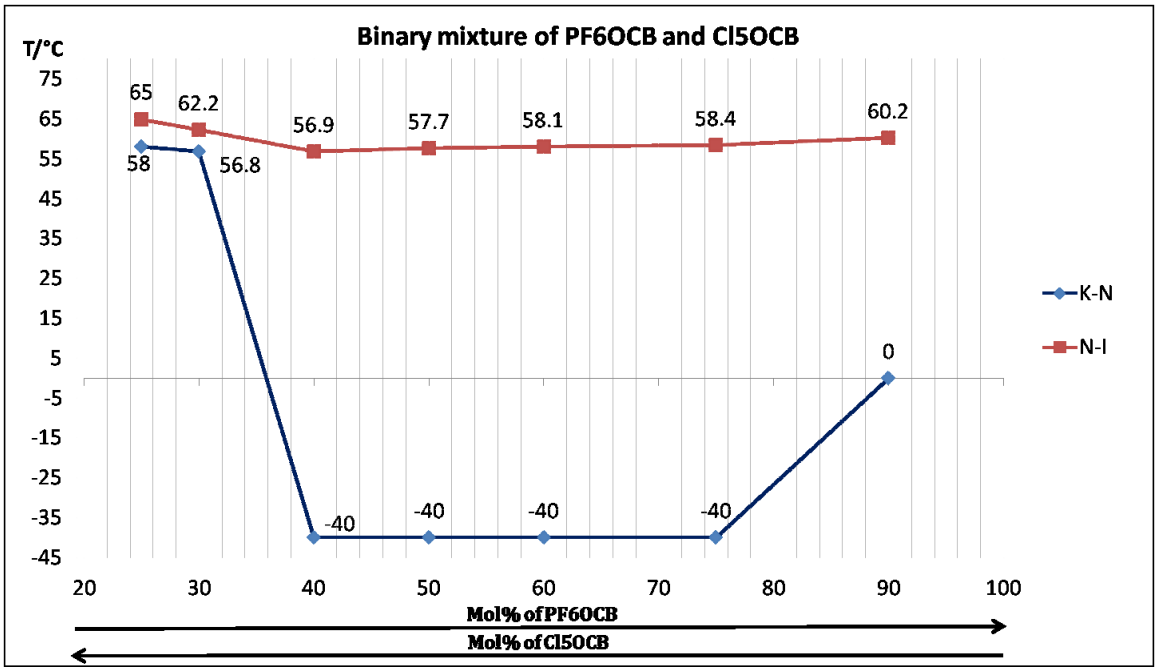

Figure 12. The phase behavior data of the binary mixtures of PF6OCB and Cl5OCB. The temperature plateau at -40 °C is an artifact due to the limitation of the DSC.

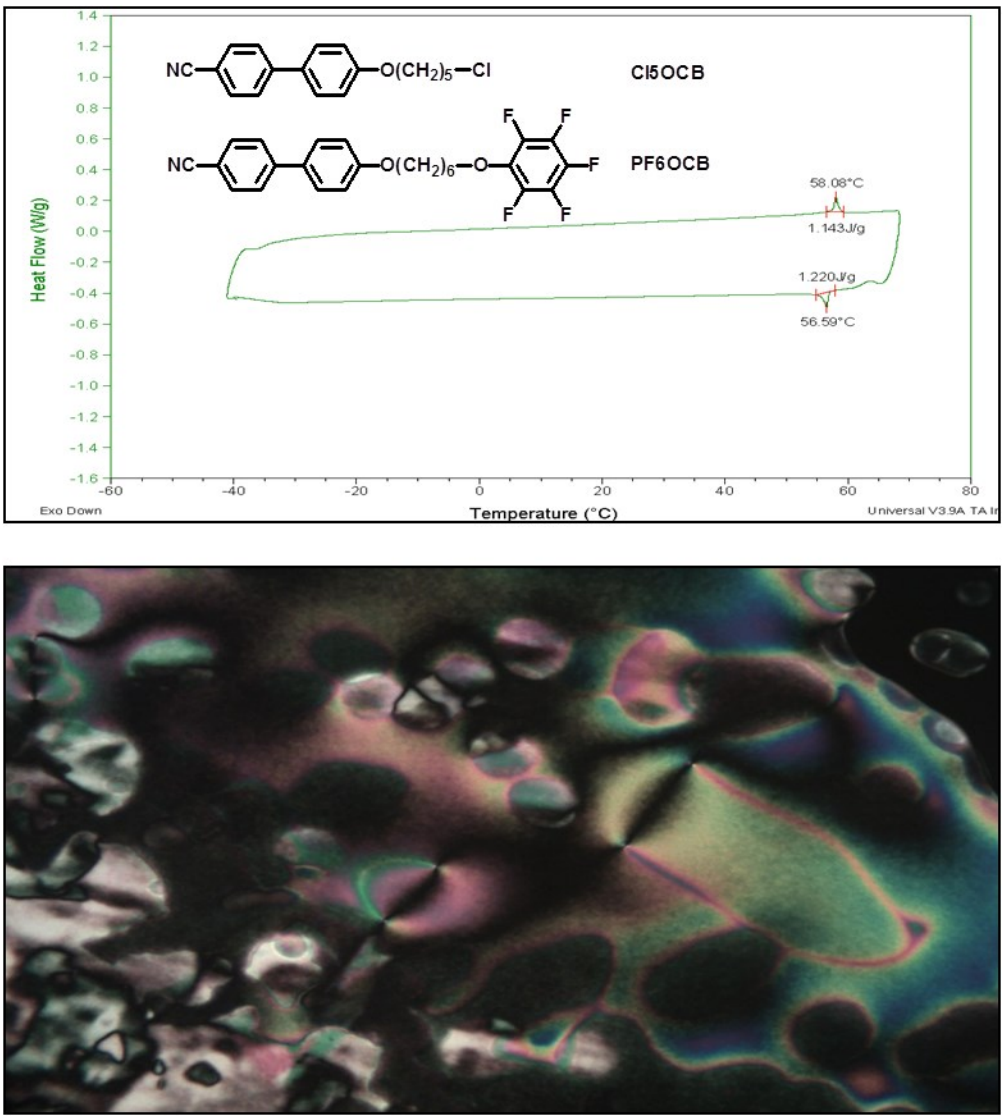

Figure 13. The DSC plot of the mixture of PF6OCB and Cl5OCB in 50%:50% molar ratio (N 58.1 I) (top) and optical microscopy image (crossed-polars) of nematic phase texture at 57 °C the transition from nematic to isotropic phase (bottom). (The lowest cooling temperature was only down to -40 °C due to the limitations of the DSC).

5. Calculations of dipole moment and binding free energy (G_{BE})

To gain more insight into the effect of the cyano-termination on the molecular properties, we calculated the dipole moments of the newly synthesized 4'-ω-cyanoalkyl-4-cyanobiphenyl, 4'-ω-cyanoalkoxy-4-cyanobiphenyl, and 4'-ω-cyanoalkoxy-4-

cyanoterphenyl compounds. Figure 14 shows the calculated dipole moments as a function of the alkyl chain length (n) (detailed results are also provided in Table SI.1). We find that the dipole moments of 4'-ω-cyanoalkyl-4-cyanobiphenyl, 4'-ω-cyanoalkoxy-4-cyanobiphenyl, and 4'-ω-cyanoalkoxy-4-cyanoterphenyl compounds follow the same qualitative trend; the dipole moment increases with increasing alkyl chain length in all three series. 4'-ω-cyanoalkoxy-4-cyanobiphenyl compounds have, however, systematically higher dipole moment than that of the corresponding 4'-ω-cyanoalkyl-4-cyanobiphenyl compound with the same alkyl chain length which reflects the effect of the electronegative O atom in the alkoxy tail. Interestingly, the dipole moment of 4'-ω-cyanoalkoxy-4-cyanobiphenyl and 4'-ω-cyanoalkoxy-4-cyanoterphenyl compounds are very similar, within ~0.1D on average, suggesting that the introduction of the third phenyl ring has a minor effect on the dipole moment relative to the analogous biphenyls.

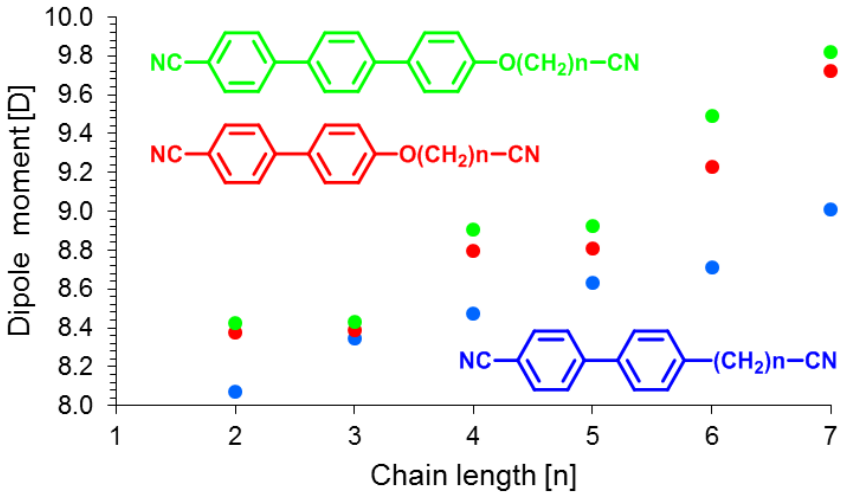

Figure 14. Calculated dipole moment (in Debye) as a function of chain length (n), shown in the molecular formula of each mesogen class, for 4'-ω-cyanoalkyl-4-cyanobiphenyl (blue), 4'-ω-cyanoalkoxy-4-cyanobiphenyl (red), and 4'-ω-cyanoalkoxy-4-cyanoterphenyl (green) compounds.

To understand more about the interfacial ordering of the cyano-terminated mesogens that are relevant for sensor applications, we calculated the G_{BE} of the 4'-ω-cyanoalkyl-4-cyanobiphenyl, 4'-ω-cyanoalkoxy-4-cyanobiphenyl, and 4'-ω-cyanoalkoxy-4-cyanoterphenyl compounds on $Al(ClO_4)_3$, $Ga(ClO_4)_3$, and $Ni(ClO_4)_2$ metal salts (see details in the computational methods section). All calculated results can be found in Table. SI.2. As there are two cyano tails in each molecule, we probe both tails to find the strongest binding functional group in all compounds. We find that in all cases (within rounding error of 0.01 eV) that the cyanobiphenyl tail binds slightly stronger than or comparable to the cyano on the alkyl tail suggesting that both ends can competitively bind to metal salt surfaces or the cyanobiphenyl tail dominates the surface. We find the largest G_{BE} difference in the case of 4'-ω-cyanoethoxy-4-cyanobiphenyl binding to $Al(ClO_4)_3$ where the cyanobiphenyl tail binds -0.22 eV stronger than that of the cyanoethoxy tail. We note here that 0.06 eV difference in G_{BE} at room temperature results in one order of magnitude difference in equilibrium constant thus -0.22 eV difference indicates the complete dominance of cyanobiphenyl tail on the surface.

We also analyze the change in G_{BE} with different lengths of the alkyl chain. G_{BE} does not show any change as a function of the alkyl chain length within rounding error (0.01 eV) for of the cyanobiphenyl tail. This result is consistent with our previous findings for hydroxyl and fluorine terminated mesogens [13, 14] and that PhCN can be used as a rational surrogate of 4'-pentyl-4-cyanobiphenyl (5CB) in G_{BE} calculations [4, 5, 13, 14, 30, 31]. Interestingly, there is significant change in G_{BE} as a function of the alkyl chain length for the cyanoalkoxy tail. For the smallest alkyl chain length (n=2), the binding of cyanoalkoxy tail is weak. The binding becomes stronger with increasing alkyl

chain length until it saturates. We suggest that this effect is the consequence of the presence of the electronegative oxygen atom in the molecular structure because in the case of cyanoalkyl tail we do not observe any change in G_{BE} as a function of alkyl chain length. Additionally, the effect of the oxygen atom on the cyano group of the cyanoalkyl tail disappears with increasing alkyl chain length which can explain the saturation in G_{BE} at long alkyl chain lengths.

Finally, we also compare the G_{BE} of mesogens related to different metal salts. We find that all three series of 4'-ω-cyanoalkyl-4-cyanobiphenyl, 4'-ω-cyanoalkoxy-4-cyanobiphenyl, and 4'-ω-cyanoalkoxy-4-cyanoterphenyl compounds bind similarly, within rounding error of 0.01 eV, to the same metal salt. This is consistent with the discussion above and that PhCN is an adequate surrogate molecule of 5CB. We do see, however, difference between the G_{BE} of mesogens related to different metal salts. G_{BE} of each cyano-terminated mesogen is -0.45, -0.56, and -1.06 eV for $Al(ClO_4)_3$, $Ga(ClO_4)_3$, and $Ni(ClO_4)_2$ metal salts, respectively, which is similar to what we have found for fluorine terminated mesogens [14]. Based on previous results [5, 30, 31], negative G_{BE} predicts homeotropic alignment at the mesogen-metal salt interface.

6. Anchoring of LCs supported on metal salts surfaces

Guided by the computational prediction that 4'-ω-cyanoalkoxy-4-cyanobiphenyl binds strongly with metal cation perchlorate salts and that they should adopt homeotropic (perpendicular) ordering, we performed the experiments using LC cells composed of two identically prepared metal salt-decorated surfaces to eliminate the confounding influence of LC-air interface on the orientation of LC. The experimental methods in this section can be found in our previous work. [30] Consistent with the negative G_{BE} values (around

-1 eV for binding with $Ni(ClO_4)_2$), CN4OCB, CN5OCB, and the mixture of CN5OCB and CN7OCB in 50%:50% molar ratio adopted homeotropic (perpendicular) ordering on surfaces supported with $Ni(ClO_4)_2$ metal salts individually (Figure 15 a). Moreover, we hypothesize that the nitrile substituted chain may perturb the smetic layer at the air interface, thus the LC anchoring at the LC-air interface would assume a parallel (planar) orientation. [38] To study this anchoring at the LC-air interface, we filled single LCs or LC mixtures in copper-TEM grids with bottom surfaces coated with 94.4±2.5 pmol/mm^2 $Ni(ClO_4)_2$ metal salts, leaving the top surface exposed to air. We observed bright cross-polarized images for all samples (CN4OCB, CN5OCB, and the mixture of CN5OCB and CN7OCB in 50%:50% molar ratio) in TEM grids (Figure 15 b). This observation suggests that the LC anchoring at the LC-air interface is planar, because the anchoring of LC at LC-metal salts surface is controlled to be homeotropic that was confirmed in LC cell setup. Additionally, a 5CB (K series with n=5) was tested in both LC cell and TEM grid setups in our past study [30]. The 5CB adopts hometotropic ordering at both the LC-$Ni(ClO_4)_2$ interface and the LC-air interface. This validates the idea that the nitrile substituted chain has an influence on anchoring at LC-air interface. In terms of pentafluorophenyloxy or chlorine tail terminated LCs, we also performed the similar anchoring test on $Ni(ClO_4)_2$-coated surfaces (SI.6). Similar to CNxOCB LCs, the mixture of PF6OCB and Cl5OCB in 50%:50% molar ratio has homeotropic anchoring at $Ni(ClO_4)_2$ surface but has planar anchoring at LC-air interface.

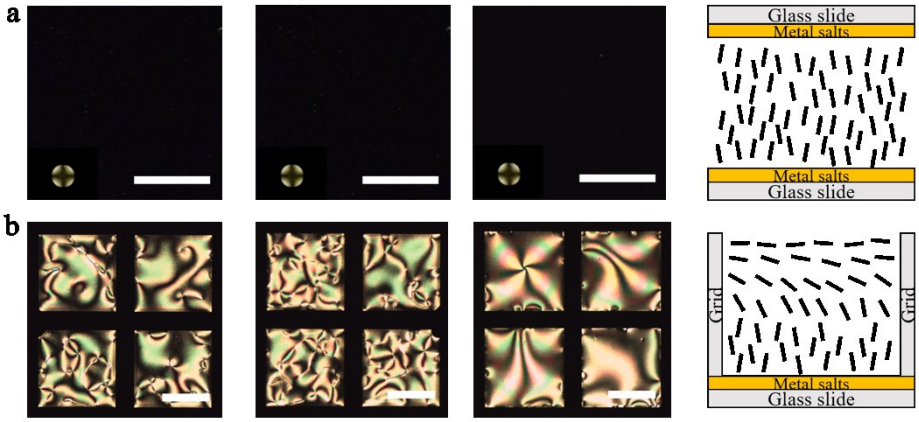

Figure 15. Cross-polarized images of CN4OCB, CN5OCB, and the mixture of CN5OCB and CN7OCB in 50%:50% molar ratio, schematic illustration of the experimental setup and LC director profile (a) when it is sandwiched between two $Ni(ClO_4)_2$ salt-decorated glass interfaces with surface density of 94.4±2.5 pmol/mm^2 or (b) when it is confined between a $Ni(ClO_4)_2$ -decorated surface with surface density of 94.4±2.5 pmol/mm^2 and an air interface. The scale bars represent 200 μm.

6. Conclusions

In this work the synthesis and mesogenic properties of a series of cyano tail terminated alkoxy and alkyl CB and CT compounds was presented. Comparison with the non-functionalized K series and M series indicates that terminal cyano group generally increases the K-N transition temperatures and the clearing points but also enhances the supercooling properties. Furthermore, a series of binary LC mixtures formed by the terminal functionalized compounds were investigated and found exhibiting promising room temperature nematic phases with wide ranges. Based on the G_{BE} values we calculated, the cyano tail terminated LCs were found adopting homeotropic ordering on surfaces supported with $Ni(ClO_4)_2$ metal salts. Moreover, the nitrile substituted chain perturbs the formation of smetic layers of molecules and leads to planar anchoring at the air interface. Further anchoring study of these materials is on the way.

Acknowledgements

This work was supported by the National Science Foundation (DMREF grant DMR-1435195) and the Army Research Office (W911NF-14-1-0140). Part of the computational work conducted by T.S. and M.M. in this study was carried out through external computational resource facilities at: the DoD High Performance Computing Modernization Program (US Air Force Research Laboratory DoD Supercomputing Resource Center (AFRL DSRC), the US Army Engineer Research and Development Center (ERDC), and the Navy DoD Supercomputing Resource Center (Navy DSRC), ARONC43623362), supported by the Department of Defense; the National Energy Research Scientific Computing Center (NERSC) through the U.S. DOE, Office of Science under Contract No. DE-AC02-05CH11231; and the Center for Nanoscale Materials (CNM) at Argonne National Laboratory (ANL) through the U.S. DOE, Office of Science under Contract No. DE-AC02-06CH11357.

References

1. Gray GW, Harrison KJ, Nash JA. New family of nematic liquid crystals for displays. Electron Lett. 1973; 9(6): 130–131.
2. Coates D. Polymer-dispersed liquid crystals. J Mater Chem. 1995; 5(12): 2063–2072.
3. Bahadur B. Liquid Crystal Displays. Mol Cryst Liq Cryst. 1984; 109(1): 3–93.
4. Szilvási T, Roling LT, Yu H, et al. Design of chemoresponsive liquid crystals through integration of computational chemistry and experimental studies. Chem Mater. 2017; 29(8): 3563–3571.
5. Szilvási T, Bao N, Nayani K, et al. Redox-triggered orientational responses of liquid crystals to chlorine gas. Angew Chem Int Ed. 2018; 57(31): 9665–9669.
6. Chan LKM, Gray GW, Lacey D. Synthesis and evaluation of some 4,4"-disubstituted lateral fluoro-1,1':4,1"-terphenyls. Mol Cryst Liq Cryst. 1985; 123(1–4): 185–204.
7. Gray GW, Hird M, Lacey D, et al. The synthesis and transition temperatures of some 4,4"-dialkyl- and 4,4"-alkoxyalkyl-1,1':4',1"-terphenyls with 2,3- or 2',3'-difluoro substituents and of their biphenyl analogs. J Chem Soc Perkin Trans 2. 1989; (12): 2041–2053.
8. Gray GW, Hird M, Toyne KJ. The synthesis and transition temperatures of some lateral monofluoro-substituted 4,4"-dialkyl- and 4,4"-alkoxyalkyl-1,1':4',1"-terphenyls. Mol Cryst Liq Cryst. 1991; 195(1): 221–237.

9. Aziz N, Kelly SM, Duffy W, et al. Rod-shaped dopants for flexoelectric nematic mixtures. Liq Cryst. 2009; 36(5): 503–520.
10. Goodby JW, Saez IM, Cowling SJ, et al, Transmission and amplification of information and properties in nanostructured liquid crystals. Angew Chem Int Ed. 2008; 47(15): 2754–2787.
11. Rupar I, Mulligan KM, Roberts JC, et al. Elucidating the smectic A-promoting effect of halogen end-groups in calamitic liquid crystals. J Mater Chem C. 2013; 1(23): 3729–3735.
12. Davis EJ, Mandle RJ, Russell BK, et al. Liquid-crystalline structure–property relationships in halogen-terminated derivatives of cyanobiphenyl. Liq Cryst. 2014; 41(11): 1635–1646.
13. Wang K, Jirka M, Rai P, et al. Synthesis and properties of hydroxy tail-terminated cyanobiphenyl liquid crystals. Liq Cryst. 2019; 46(3): 397–407.
14. Wang K, Rai P, Fernando A, et al. Synthesis and properties of fluorine tail-terminated cyanobiphenyls and terphenyls for chemoresponsive liquid crystals. Liq Cryst. 2019; DOI:10.1080/02678292.2019.1616228.
15. Mandle RJ, Davis EJ, Voll C-CA, et al. Self-organisation through size-exclusion in soft materials. J Mater Chem C. 2015; 3(10): 2380–2388.
16. Adomenas P, Butkus V, Daugvila J, et al. Acetylenic liquid crystals available by Castro reaction. In: Bata L. Editor. Proceedings of the Third Liquid Crystal Conference of the Socialist Countries; 1979 Aug 27–31; Budapest. Oxford: Pergamon Press; 1980. p. 1029–1038
17. Daugvila J, Tubalyte A, Denys G, et al. Liquid crystals of α-cyanostilbene type. Zh Obshch Khim. 1976; 46 (9): 2125–2130.
18. Rjumtsev EI, Kovshik AP. Effect of aliphatic spacers on electrooptical and dielectric properties of strongly polar liquid crystals, Mol Cryst Liq Cryst. 1990; 191(1): 321–325.
19. Ostrovskii BI, Saidachmetov MA, X-ray study of modulated smectic A phase, Mol Cryst Liq Cryst Incorporating Nonlinear Optics. 1990; 192(1):19–24.
20. Barbarin F, Dugay M, Oukarfi B. Polar smectogens: polymorphism of some cyanoalkoxybiphenylalkoxybenzoates and related compounds. Liq Cryst. 1992; 11(2): 219–234.
21. Barbarin F, Dugay M, Piovesan A, et al. Phase transitions between single- and double-layered smectic structures in binary mixtures of cyano-mesogens. J de Phys. 1988; 49 (9):1583–1591.

22. Katagiri T, Ota S, Ohira T, et al. Synthesis of thiophene/phenylene co-oligomers. V. Functionalization at molecular terminals toward optoelectronic device applications. J Hetero Chem. 2007; 44(4): 853–862.
23. Chen L, Chen Y, Zhou W, et al. Synthesis and properties of light-emitting polythiophene derivatives bearing terphenyl mesogenic pendant. Mol Cryst Liq Cryst. 2010; 518(1): 70–83.
24. Frisch MJ, Trucks GW, Schlegel HB, et al. Gaussian 09, Revision D.01, Gaussian, Inc., Wallingford CT, 2009.
25. Perdew JP, Burke K, Ernzerhof M. Generalized gradient approximation made simple. Phys Rev Lett. 1996; 77(18): 3865–3868.
26. Grimme S, Antony J, Ehrlich S, et al. A consistent and accurate ab initio parametrization of density functional dispersion correction (DFT-D) for the 94 elements H-Pu. J Chem Phys. 2010; 132: 154104/1–154104/19.
27. Marenich AV, Cramer CJ, Truhlar DG. Universal solvation model based on solute electron density and on a continuum model of the solvent defined by the bulk dielectric constant and atomic surface tensions. J Phys Chem B. 2009; 113(18) 6378–6396.
28. Weigend F, Ahlrichs R. Balanced basis sets of split valence, triple zeta valence and quadruple zeta valence quality for H to Rn: Design and assessment of accuracy. Phys Chem Chem Phys. 2005; 7(18): 3297–3305.
29. Zhao Y, Truhlar DG. The M06 suite of density functionals for main group thermochemistry, thermochemical kinetics, noncovalent interactions, excited states, and transition elements: two new functionals and systematic testing of four M06-class functionals and 12 other functionals. Theor Chem Acc. 2008; 120(1–3): 215–241.
30. Szilvási T, Bao N, Yu H, et al. The role of anions in adsorbate-induced anchoring transitions of liquid crystals on surfaces with discrete cation binding sites. Soft Matter. 2018; 14(5): 797–805.
31. Yu H, Szilvási T, Rai P, et al. Computational chemistry-guided design of selective chemoresponsive liquid crystals using pyridine and pyrimidine functional groups. Adv Funct Mater. 2018; 28(13): 1703581/1–1703581/10.
32. Mandle RJ, Stevens MP, Goodby JW. Developments in liquid-crystalline dimers and oligomers. Liq Cryst. 2017; 44(12–13): 2046–2059.
33. Itahara T. Effect of the pentafluorophenyloxy group on liquid crystalline behaviour. Liq Cryst. 2005; 32(1): 115–118.

34. Constant J, Raynese EP. Flow Aligned Viscosities of Cyanobiphenyls. Mol Cryst Liq Cryst. 1980; 62(1-2): 115–123.
35. Zang Z, Zhang D, Wan X, et al. The Synthesis and property of liquid crystalline 4-alkoxyl-4″-cyano-p-terphenyls. Mol Cryst Liq Cryst. 2000; 339(1): 145–158.
36. Roman Yu Peshkov, Elena V Panteleeva, Wang Chunyan, Evgeny V Tretyakov and Vitalij D Shteingarts. One-pot synthesis of 4′-alkyl-4-cyanobiaryls on the basis of the terephthalonitrile dianion and neutral aromatic nitrile cross-coupling. Beilstein J Org Chem. 2016; 12: 1577–1584.
37. Daniel MF, Lettington OC, Small SM. Langmuir-Blodgett Films of Amphiphiles with Cyano Headgroups. Mol Cryst Liq Cryst. 1983; 96(1): 373–386.
38. Nayani K, Rai P, Bao N, et al. Liquid crystals with interfacial ordering that enhances responsiveness to chemical targets. Adv Mat. 2018; 30(27): 1706707/1–1706707/7.

Supporting Information

New room temperature nematogens by cyano tail termination of alkoxy and alkylcyanobiphenyls and their anchoring behavior on metal salt-decorated surface

Kunlun Wang[a], Tibor Szilvási[b], Jake I. Gold[b], Huaizhe Yu[c], Nanqi Bao[c], Prabin Rai[a], Manos Mavrikakis[b], Nicholas L. Abbott[c], and Robert J. Twieg[a*]

[a]Department of Chemistry and Biochemistry,

Kent State University, Kent, OH 44242 USA

[b]Department of Chemical and Biological Engineering,

University of Wisconsin-Madison, Madison, WI 53706 USA

[c] Department of Chemical and Biomolecular Engineering, Cornell

University, Ithaca, NY14853 USA

* Author for Correspondence: rtwieg@kent.edu

Table of Contents

SI.1 Synthesis of cyano tail-terminated cyanobiphenyl/terphenyl compounds 3

SI.2 Synthesis of PF6OCB 14

SI. 3 The NMR spectra of representative compounds 16

SI. 4 The DSC plots of the cyano tail terminated liquid crystals that are not shown in main text. (The second heating cooling cycle is shown for all cases) 27

SI.5. Dipole moment and Gibbs Free Energy of adsorption for cyano-terminated compounds 30

SI.6. Anchoring Study of the Binary Mixtures of PF6OCB and Cl5OCB in 50%:50% Molar Ratio on $Ni(ClO_4)_2$-Coated Surfaces and Air Free Interface 31

SI.1 Synthesis of cyano tail-terminated cyanobiphenyl/terphenyl compounds

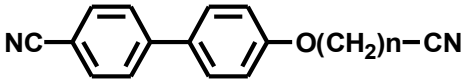

n = 2, CN2OCB (using acrylonitrile)

In a 200 ml recovery flask with stirbar was placed 4-hydroxycyanobiphenyl (1.95 gm, 10.0 mmol), acrylonitrile (20 ml), *t*-BuOH (30 mg, 0.04 mmol) and DMAP (50 mg, 0.04 mmol). The flask was fitted with a bump trap as condenser and the mixture was heated with stirring in a 90°C oil bath for 72 hours (after which time only a small amount of starting material remained). The mixture was stirred in an ice water bath and 2% aqueous HCl was added dropwise with stirring to fill the flask. A solid precipitate appeared and after stirring 15 min in the ice bath it was collected by suction filtration, washed well with water and air dried. This material was taken up in boiling methanol which was hot filtered. Upon cooling crystals appeared which were collected by suction filtration, washed with cold ethanol and air dried. The product was collected as white needle crystals in two crops totaling 2.17 gm (88%). MP: 186 °C. ^{1}H NMR (400 MHz, $CDCl_3$) δ (ppm): 7.71-7.61 (m, 4H), 7.52 (td, ^{1}J = 8.4 Hz, ^{2}J = 1.6 Hz, 2H), 6.98 (td, ^{1}J = 8.8 Hz, ^{2}J = 2.0 Hz, 2H), 4.26 (t, J = 6.4 Hz, 2H), 2.86 (t, J = 6.4 Hz, 2H); ^{13}C NMR (100 MHz, $CDCl_3$) δ (ppm): 158.6, 144.9, 132.9, 132.6, 128.6, 127.2, 118.8, 116.1, 115.4, 110.1, 62.9, 18.6; IR (cm^{-1}): 2972, 2938, 2249, 2224, 1602, 1494, 1241, 1181, 813.

General Procedure A for the synthesis of cyano tail-terminated alkoxy cyanobiphenyl compounds (n = 3-6)

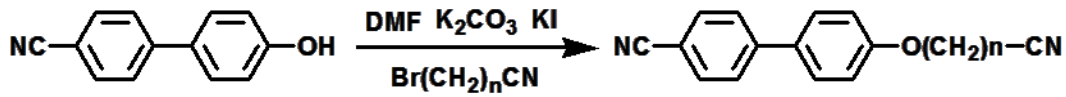

In a 200 ml round bottom flask was placed 4-cyano-4'-hydroxybiphenyl (1.0 equiv.), α,ω-bromoalkylnitrile (1.0 equiv.), dry DMF (1.0 ml per 1.0 mmol substrate), potassium carbonate (2.0 equiv.) and potassium iodide (0.1 equiv.). The resulting suspension was stirred overnight at room temperature and the reaction was monitored by TLC analysis. Upon completion, water was added dropwise with stirring to fill the flask and then the precipitate was collected by vacuum filtration. In some cases when no precipitate was found, the mixture was extracted with dichloromethane. The crude product was recrystallized from methanol.

n = 3, CN3OCB (by General Procedure A)

2.11 g, 81% yield after recrystallization from methanol.

^{1}H NMR (400 MHz, $CDCl_3$) δ (ppm): 7.69 (d, *J* = 8.0 Hz, 2H), 7.63 (d, *J* = 8.4 Hz, 2H), 7.53 (td, ^{1}J = 8.8 Hz, ^{2}J = 3.2 Hz, 2H), 7.00 (td, ^{1}J = 9.2 Hz, ^{2}J = 2.8 Hz, 2H), 4.14 (t, *J* = 6.0 Hz, 2H), 2.63 (t, *J* = 7.2 Hz, 2H), 2.18 (m, 2H); ^{13}C NMR (100 MHz, $CDCl_3$) δ (ppm): 159.0, 145.1, 132.6, 132.1, 128.5, 127.2, 119.1, 115.1, 110.3, 65.4, 25.4, 14.2. IR (cm^{-1}): 2937, 2876, 2246, 2225, 1602, 1494, 1244, 1183, 826. GC-MS: 262.25 found 262.31 calc. POM: K 138 I 79 N 71 K

DSC: K 137.9 I 79.0 N 70.9 K

n = 4, CN4OCB (by General Procedure A)

870 mg, 63% yield after recrystallization from methanol.

^{1}H NMR (400 MHz, $CDCl_3$) δ (ppm): 7.70 (td, ^{1}J = 8.0 Hz, ^{2}J = 0.8 Hz, 2H), 7.64 (td, ^{1}J = 8.0 Hz, ^{2}J = 0.8 Hz, 2H), 7.53 (td, ^{1}J = 8.8 Hz, ^{2}J = 2.8 Hz, 2H), 6.99 (td, ^{1}J = 8.8 Hz, ^{2}J = 2.8 Hz, 2H), 4.07 (t, J = 6.0 Hz, 2H), 2.47 (t, J = 6.8 Hz, 2H), 2.01-1.90 (m, 4H); ^{13}C NMR (100 MHz, $CDCl_3$) δ (ppm): 159.3, 145.1, 132.6, 131.8, 128.4, 127.1, 119.5, 119.1, 115.0, 110.2, 66.8, 28.2, 22.4, 17.1. IR (cm^{-1}): 2937, 2876, 2243, 2221, 1601, 1493, 1249, 1179, 827. GC-MS: 276.24 found 276.33 calc.
DSC: K 93.1 I 61.2 N 37.8 K

POM: K 93 I 62 N 28 K

n = 5, CN5OCB (by General Procedure A)

1.0 g, 69% yield after recrystallization from methanol.

^{1}H NMR (400 MHz, $CDCl_3$) δ (ppm): 7.69 (td, ^{1}J = 8.4 Hz, ^{2}J = 1.6 Hz, 2H), 7.64 (dd, ^{1}J = 8.0 Hz, ^{2}J = 1.2 Hz, 2H), 7.53 (td, ^{1}J = 8.8 Hz, ^{2}J = 3.2 Hz, 2H), 6.99 (td, ^{1}J = 8.8 Hz, ^{2}J = 2.0 Hz, 2H), 4.03 (t, J = 6.0 Hz, 2H), 2.40 (t, J = 6.8 Hz, 2H), 1.85 (m, 2H), 1.79-1.65 (m, 4H); ^{13}C NMR (100 MHz, $CDCl_3$) δ (ppm): 159.5, 145.2, 132.6, 131.5, 128.4, 127.1, 119.6, 119.1, 115.1, 110.1, 67.5, 28.5, 25.4, 25.2, 17.2. IR (cm^{-1}): 2950, 2909, 2872, 2244, 2223, 1600, 1494, 1246, 1180, 811. GC-MS: 290.23 found 290.36 calc.
DSC: K 65.8 N 76.7 I 75.6 N 4.9 K

POM: K 67.8 N 77.3 I 76.8 N

n = 6, CN6OCB (by General Procedure A)

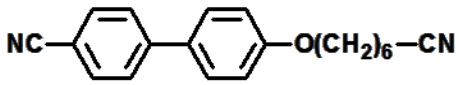

1.2 g, 79% yield after recrystallization from methanol.

^{1}H NMR (400 MHz, $CDCl_3$) δ (ppm): 7.69 (td, ^{1}J = 7.6 Hz, ^{2}J = 1.2 Hz, 2H), 7.63 (dd, ^{1}J = 6.8 Hz, ^{2}J = 2.0 Hz, 2H), 7.53 (td, ^{1}J = 6.4 Hz, ^{2}J = 5.2 Hz, 2H), 6.99 (td, ^{1}J = 8.8 Hz, ^{2}J = 2.8 Hz, 2H), 4.02 (t, J = 6.0 Hz, 2H), 2.37 (t, J = 7.2 Hz, 2H), 1.83 (m, 2H), 1.73 (m, 2H), 1.57-1.53 (m, 4H); ^{13}C NMR (100 MHz, $CDCl_3$) δ (ppm): 159.6, 145.2, 132.6, 131.4, 128.4, 127.1, 119.7, 119.1, 115.1, 110.1, 67.8, 28.9, 28.4, 25.4, 25.3, 17.1. IR (cm^{-1}): 2935, 2856, 2247, 2224, 1600, 1493, 1181, 818. GC-MS: 304.32 found 304.39 calc.
DSC: K 97.1 I 68.3 K

POM: K 97 I

n = 5, Cl5OCB (by General Procedure A)

1-Bromo-5-chloropentane (5.0 mmol, 927 mg) was used. White crystals recrystallized from methanol. (890 mg, yield: 60%)

^{1}H NMR (400 MHz, $CDCl_3$) δ (ppm): 7.70 (m, 2H), 7.64 (m, 2H), 7.53 (td, ^{1}J = 8.8 Hz, ^{2}J = 2.8 Hz, 2H), 6.99 (td, ^{1}J = 8.8 Hz, ^{2}J = 2.8 Hz, 2H), 4.03 (t, J = 5.6 Hz, 2H), 3.58 (t, J = 6.8 Hz, 2H), 1.91-1.82 (m, 4H), 1.65 (m, 2H); ^{13}C NMR (100 MHz, $CDCl_3$) δ (ppm): 159.3, 145.2, 132.6, 131.4, 128.4, 127.1, 119.1, 115.1, 110.1, 67.8, 44.9, 32.3, 28.5, 23.5. GC-MS:299.18 found 299.79 calc.

Synthesis of the cyano tail terminated compounds CN7OCB, CN5CB, CB6CB and CN7CB was accomplished by substitution of the relevant hydroxy tail terminated intermediates. (General Procedure B)

4'-[(7-Hydroxyheptyl)oxy]-4-cyanobiphenyl

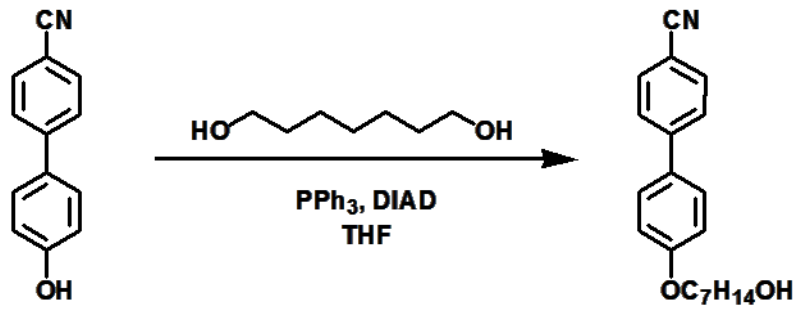

In a 100 ml round bottom flask with stirbar was placed 4'-hydroxy-4-cyanobiphenyl (2.7 g, 13.8 mmol), triphenylphosphine (4.5 g, 16.5 mmol), 1,7-heptanediol (2.2 g, 16.5 mmol) and dry THF (25 ml). The resulting solution was chilled in an ice bath and diethylazodicarboxylate (94%, 3.5 g, 16.5 mmol) was added in portions over ten minutes. The mixture was allowed to warm to room temperature and monitored by TLC until completion. The mixture was allowed to stir overnight, and the reaction was terminated by addition of silica gel and the mixture was concentrated to dryness. The adsorbed material was placed at the top of a column made up with 20% ethyl acetate / 80% hexanes and eluted with a gradient up to ethyl acetate and hexanes (1:4). Fractions containing only the desired product were combined and concentrated to give the desired product as a white solid (2.4 g, 56%).

^{1}H NMR (400 MHz, $CDCl_3$) δ (ppm): 7.68 (dd, ^{1}J = 6.4 Hz, ^{2}J = 1.6 Hz, 2H), 7.63 (dt, ^{1}J = 8.0 Hz, ^{2}J = 1.6 Hz, 2H), 7.51 (dd, ^{1}J = 7.2 Hz, ^{2}J = 2.4 Hz, 2H), 6.98 (d, J = 8.8 Hz, 2H), 3.99 (t, J = 6.8 Hz, 2H), 3.65 (t, J = 6.4 Hz, 2H), 1.81 (m, 2H), 1.58 (q, J = 2.4 Hz, 2H), 1.51-1.40 (m, 6H); ^{13}C NMR (100 MHz, $CDCl_3$) δ (ppm): 159.8, 145.3, 132.6, 131.3, 128.3, 127.1, 119.2, 115.1, 110.0, 68.1, 62.9, 32.7, 29.2, 26.0, 25.7.

4'-[[7-[[(4-methylphenyl)sulfonyl]heptyl]oxyl]-4-cyanobiphenyl

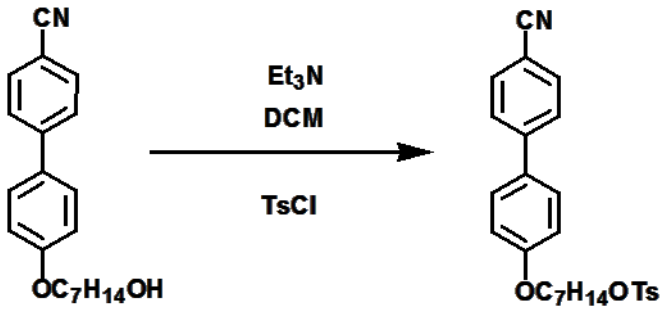

A 100 mL flask was charged with 4'-[(7-hydroxyheptyl)oxy]-4-cyanobiphenyl (2.0 g, 6.7 mmol), triethylamine (0.89 g, 8.7 mmol) and DCM (6.0 mL). The mixture was cooled to a temperature of about 5°C to 15°C and cautiously charged with a solution of *p*-toluenesulfonyl chloride (1.28 g, 6.7 mmol) in DCM (5.0 mL) over 30 minutes via additional funnel. Once the addition was complete, the reaction mixture was warmed to

18 °C to 22 °C and stirred for 12 hours. To this solution was added 6N hydrochloric acid (0.55 mL) cautiously while maintaining temperature below 25 °C. The aqueous phase was removed, and the organic phase was washed with water and dried over magnesium sulfate. The product was purified by column chromatography to afford a low melting white solid (Yield: 2.1 g, 68%)

^{1}H NMR ($CDCl_3$, 400 MHz) δ (ppm): 7.78 (dt, ^{1}J = 6.4 Hz, ^{2}J = 2.0 Hz, 2H), 7.69-7.63 (m, 4H), 7.51 (m, 2H), 7.34 (m, 2H), 6.98 (m, 2H), 4.02 (m, 4H), 2.44 (s, 3H), 1.73 (m, 2H), 1.41 (m, 2H), 1.34-1.26 (m, 6H); ^{13}C NMR ($CDCl_3$, 100 MHz) δ (ppm): 159.7, 145.3, 144.7, 133.2, 132.6, 131.3, 129.8, 128.4, 127.9, 127.1, 119.2, 115.1, 110.2, 70.6, 68.0, 29.1, 28.8, 28.7, 25.8, 25.3, 21.7.

n = 7, CN7OCB

To a solution of 4'-[[7-[[(4-methylphenyl)sulfonyl]heptyl]oxyl]-4-cyanobiphenyl (1.1 g, 3.0 mmol) in DMSO (15 mL) was added NaCN (186 mg, 3.8 mmol). The mixture was stirred for 8 hours at 60 °C then at room temperature overnight. The residue was diluted with water (30 mL) and extracted with diethyl ether (15 mL). The organic phase was dried over magnesium sulfate and evaporated under reduced pressure. The desired product was separated by column chromatography eluted by ethyl acetate:hexane (1:4) as white crystals, which was then recrystallized from methanol as a white solid. (Yield: 440 mg, 46%)

^{1}H NMR ($CDCl_3$, 400 MHz) δ (ppm): 7.69 (td, ^{1}J = 8.0 Hz, ^{2}J = 0.8 Hz, 2H), 7.64 (td, ^{1}J = 8.0 Hz, ^{2}J = 1.2 Hz, 2H), 7.53 (td, ^{1}J = 8.8 Hz, ^{2}J = 2.4 Hz, 2H), 6.99 (dd, ^{1}J = 6.4 Hz, ^{2}J = 2.0 Hz, 2H), 4.01 (t, J = 6.4 Hz, 2H), 2.36 (t, J = 7.2 Hz, 2H), 1.82 (m, 2H), 1.69 (m, 2H), 1.52 (m, 4H), 1.43 (m, 2H); ^{13}C NMR ($CDCl_3$, 100 MHz) δ (ppm): 160.1, 145.7, 133.0, 132.9, 131.8, 128.7, 128.5, 119.5, 115.5, 110.5, 68.3, 29.5, 29.0, 28.9, 28.8, 26.2, 25.7, 17.5; IR (cm^{-1}): 2933, 2866, 2246, 2219, 1600, 1494, 1248, 1179, 817; GC/MS: 318.25 found 318.41 calc.

POM: K 60.8 N 70.8 I 70.7 N 27 I

The cyanoalkyl cyanobiphenyl compounds (n = 5-7) were synthesized by General Procedure B.

n = 5, CN5CB (by General Procedure B)

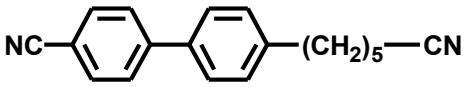

800 mg, 80% yield. A white solid.

^{1}H NMR ($CDCl_3$, 400 MHz) δ (ppm): 7.72 (td, ^{1}J = 8.0 Hz, ^{2}J = 0.8 Hz, 2H), 7.66 (td, ^{1}J = 8.0 Hz, ^{2}J = 1.2 Hz, 2H), 7.52 (td, ^{1}J = 8.8 Hz, ^{2}J = 2.4 Hz, 2H), 7.28 (dd, ^{1}J = 6.4 Hz, ^{2}J = 2.0 Hz, 2H), 2.69 (t, J = 7.6 Hz, 2H), 2.35 (t, J = 7.2 Hz, 2H), 1.69 (m, 4H), 1.54 (m, 2H); ^{13}C NMR ($CDCl_3$, 100 MHz) δ (ppm): 145.5, 142.8, 136.8, 132.6, 129.2, 127.5, 127.2, 119.7, 119.0, 110.6, 35.3, 30.5, 28.3, 25.3, 17.1;

POM: K 65.8 I 25 K

n = 6, CN6CB (by General Procedure B)

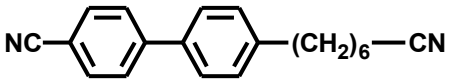

32 mg, recrystallized from methanol, 40% yield.

^{1}H NMR ($CDCl_3$, 400 MHz) δ (ppm): 7.71 (td, ^{1}J = 8.0 Hz, ^{2}J = 0.8 Hz, 2H), 7.67 (td, ^{1}J = 8.0 Hz, ^{2}J = 1.2 Hz, 2H), 7.51 (td, ^{1}J = 8.8 Hz, ^{2}J = 2.4 Hz, 2H), 7.28 (dd, ^{1}J = 6.4 Hz, ^{2}J = 2.0 Hz, 2H), 2.68 (t, J = 7.6 Hz, 2H), 2.34 (t, J = 6.8 Hz, 2H), 1.66 (m, 4H), 1.50 (m, 2H), 1.42 (m, 2H); ^{13}C NMR ($CDCl_3$, 100 MHz) δ (ppm): 145.5, 143.2, 136.7, 132.6, 129.2, 127.5, 127.2, 119.7, 119.0, 110.6, 35.4, 31.0, 28.5, 28.4, 25.3, 17.1; IR (cm^{-1}): 2935, 2857, 2247, 2226, 1605, 1494, 812; GC/MS: 288.26 found 288.39 calc.

DSC; K 61 I 35 N -7 K

POM: K 60 I 34 N

n = 7, CN7CB (by General Procedure B)

07033KW

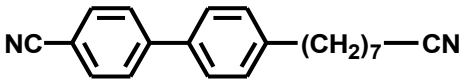

29 mg, recrystallized from methanol, 24% yield.

^{1}H NMR ($CDCl_3$, 400 MHz) δ (ppm): 7.71 (td, ^{1}J = 8.0 Hz, ^{2}J = 0.8 Hz, 2H), 7.67 (td, ^{1}J = 8.0 Hz, ^{2}J = 1.2 Hz, 2H), 7.50 (td, ^{1}J = 8.8 Hz, ^{2}J = 2.4 Hz, 2H), 7.28 (dd, ^{1}J = 6.4 Hz, ^{2}J = 2.0 Hz, 2H), 2.67 (t, J = 7.2 Hz, 2H), 2.34 (t, J = 7.2 Hz, 2H), 1.66 (m, 4H), 1.46 (m, 2H), 1.39 (m, 4H); ^{13}C NMR ($CDCl_3$, 100 MHz) δ (ppm): 145.6, 143.4, 136.6, 132.6, 129.2, 127.5, 127.1, 119.8, 119.0, 110.6, 35.5, 31.2, 28.9, 28.6, 28.5, 25.3, 17.1; IR (cm^{-1}): 2920, 2854, 2246, 2224, 1604, 1495, 820; GC/MS: 302.29.26 found 302..41 calc.

POM: K 66 I 36 K

Synthesis of Cyano-terminated alkoxy cyanoterphenyl compounds CNnOCT

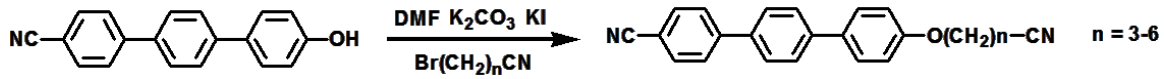

Procedure for the synthesis of 1-bromo-4-hydroxybiphenyl

4-acetoxybiphenyl. A 500 mL round bottom flask was charged with 4-phenylphenol (125 g, 0.7 mol), acetic anhydride (112.5 g, 1.1 mol), and concentrated sulfuric acid (cat.). The flask was fitted with a reflux condenser and was heated under nitrogen in an oil bath for 3 hours. Reaction progress was monitored by TLC, noting the disappearance of the

spot for 4-phenylphenol and the appearance of a single spot for the product. The flask was removed from the oil bath, and water (~400 mL) was added to precipitate the product, and the product was dried by vacuum filtration. The product was purified by recrystallization from ethanol, giving the product as a white powder (152.8 g, 98%); mp 87 °C. ^{1}H-NMR (400 MHz, $CDCl_3$): 7.62 (d, J= 8.76 Hz, 2H); 7.59 (d, J= 7.04 Hz, 2H); 7.46 (dd, J= 7.52 Hz, 7.52 Hz, 2H); 7.38 (t, J= 7.34 Hz, 1H); 7.19 (d, J= 8.68 Hz, 2H); 2.36 (s, 3H).IR (Neat): 1748, 1598, 1515, 1484, 1428, 1372, 1217, 1193, 1165, 1106, 1052, 1017, 1008, 942, 906, 850, 832, 765, 735, 967, 650 cm^{-1}.

4-bromo-4'-acetoxybiphenyl. A 500 mL round bottom flask was charged with 4-acetoxybiphenyl (100.0 g, 471.0 mmol), sodium carbonate (149.8 g, 1.4 mol), and 1,1,2,2-tetrachloroethane (100 mL). A reflux condenser was attached, and the contents of the flask were heated under nitrogen to 50 °C in an oil bath. To this solution, a solution of bromine (113.0 g, 707.0 mmol) in 1,1,2,2-tetrachloroethane (100 mL) was added dropwise and the mixture was stirred overnight. Reaction completion was observed by TLC, noting the disappearance of the spot for 4-acetoxybiphenyl and the appearance of a new spot for the product. The solvent was removed under vacuum, and the product was washed with a 10% solution of sodium thiosulfate. The product was dried by vacuum filtration, giving the crude product. The crude product was purified by recrystallization from toluene, giving the product as white crystals (118.2 g, 86%); mp 132 °C. ^{1}H-NMR (400 MHz, $CDCl_3$): 7.59 (d, 2H); 7.57 (d, 2H); 7.44 (d, 2H); 7.19 (d, 2H); 2.35 (s, 3H). IR (Neat): 1747, 1479, 1194, 1071, 1001, 908, 822, 802, 746 cm^{-1}.

4-bromo-4'-hydroxybiphenyl. A 2 L round bottom flask was charged with 4-bromo-4'-acetoxybiphenyl (38.9 g, 133.0 mmol), and sodium hydroxide (38.9 g, 972.0 mmol, in 780 mL 80% aqueous ethanol). A reflux condenser was attached, and the solution was refluxed with stirring overnight. The contents of the flask were cooled to room temperature, and the ethanol was removed by rotary evaporation. Water (~700 mL) was added to the flask to redissolve the solid products, and the solution was neutralized with

hydrochloric acid. The precipitate was collected and dried by vacuum filtration. The crude product was purified by recrystallization from a 1/4 solution of ethanol/water, giving the product as white crystals (31.1 g, 94%), mp 159 °C. NMR (400 MHz, $CDCl_3$): ^{1}H-NMR (400 MHz, $CDCl_3$): 9.63 (s, 1H); 7.57 (d, J= 8.64 Hz, 2H); 7.53 (d, J= 8.68 Hz, 2H); 7.51 (d, J= 8.64 Hz, 2H); 6.85 (d, J= 8.64 Hz, 2H). IR (Neat): 3395, 1592, 1522, 1474, 1439, 1371, 1222, 1079, 998, 810, 727 cm^{-1}.

The 4"-hydroxy-4-cyanoterphenyl was prepared by a Suzuki coupling of 1-bromo-4-hydroxybiphenyl with 4-cyanophenylboronic acid[1].

n = 3, CN3OCT (General Procedure A)

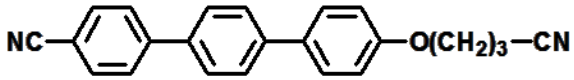

110 mg, 57% yield after recrystallization from acetonitrile.

7.72 (m, 4H), 7.66 (m, 4H), 7.58 (td, ^1J = 8.8 Hz, ^2J = 3.2 Hz, 2H), 7.00 (td, ^1J = 8.8 Hz, ^2J = 2.8 Hz, 2H), 4.15 (t, J = 5.6 Hz, 2H), 2.63 (t, J = 6.8 Hz, 2H), 2.18 (m, 2H); ^{13}C NMR (100 MHz, $CDCl_3$) δ (ppm): 158.3, 145.2, 141.0, 137.4, 133.3, 132.7, 128.2, 127.6, 127.5, 127.4, 119.0, 114.9, 110.8, 65.4, 25.5, 14.2. IR (cm^{-1}): 2949, 2927, 2877, 2251, 2225, 1597, 1487, 1254, 1045, 810. GC-MS: No peak
DSC: K 172 N 286 I 286 N 162 K

POM: K 173 N 284I 284 N 165 K

n = 4, CN4OCT (General Procedure A)

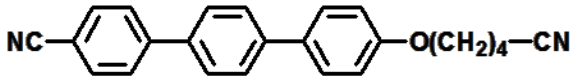

140 mg, 70% yield after recrystallization from acetonitrile.

^{1}H NMR (400 MHz, $CDCl_3$) δ (ppm): 7.73 (dt, ^1J = 8.8 Hz, ^2J = 1.2 Hz, 4H), 7.65 (m, 4H), 7.58 (td, ^1J = 8.8 Hz, ^2J = 2.8 Hz, 2H), 6.99 (td, ^1J = 8.8 Hz, ^2J = 3.2 Hz, 2H), 4.07 (t, J = 5.6 Hz, 2H), 2.48 (t, J = 6.8 Hz, 2H), 2.02-1.90 (m, 4H); ^{13}C NMR (100 MHz, $CDCl_3$) δ (ppm): 158.6, 145.2, 141.1, 137.4, 132.9, 132.7, 128.2, 127.6, 127.5, 127.3,

119.5, 119.0, 115.0, 110.8, 66.8, 28.2, 22.5, 17.0. IR (cm^{-1}): 2937, 2876, 2243, 2228, 1598, 1488, 1255, 1029, 809. GC-MS: No peak

DSC: K 141 N 269 I 269 N 134 K

POM: K 140 N 267.1 I 267.1 N 136 K

n = 5, CN5OCT (General Procedure A)

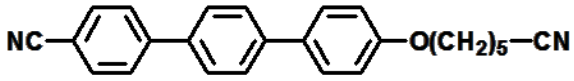

182 mg, 62% yield after recrystallization from acetonitrile.

^{1}H NMR (400 MHz, $CDCl_3$) δ (ppm): 7.72 (d, J = 9.2 Hz, 4H), 7.66 (m, 4H), 7.57 (td, ^{1}J = 8.8 Hz, ^{2}J = 3.2 Hz, 2H), 6.99 (td, ^{1}J = 9.2 Hz, ^{2}J = 3.2 Hz, 2H), 4.04 (t, J = 6.0 Hz, 2H), 2.41 (t, J = 6.8 Hz, 2H), 1.86 (m, 2H), 1.77 (m, 2H), 1.68 (m, 2H); ^{13}C NMR (100 MHz, $CDCl_3$) δ (ppm): 158.8, 145.2, 141.2, 137.3, 132.7, 132.6, 128.1, 127.6, 127.5, 127.3, 119.0, 114.9, 110.8, 67.5, 28.5, 25.4, 25.2, 17.2. IR (cm^{-1}): 2944, 2910, 2870, 2246, 2226, 1598, 1488, 1251, 808. GC-MS: No peak.
DSC: K 154 Sm 177 N 264 I 263 N 172 Sm 145 K

POM: K 155 Sm 177 N 258 I 257 N 172 Sm 145 K1 100 K

n = 6, CN6OCT (General Procedure A)

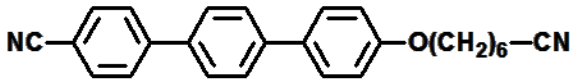

125 mg, 58% yield after recrystallization from acetonitrile.

^{1}H NMR (400 MHz, $CDCl_3$) δ (ppm): 7.71 (m, 4H), 7.66 (m, 4H), 7.57 (td, ^{1}J = 8.8 Hz, ^{2}J = 2.8 Hz, 2H), 6.99 (td, ^{1}J = 8.8 Hz, ^{2}J = 2.8 Hz, 2H), 4.02 (t, J = 6.4 Hz, 2H), 2.38 (t, J = 7.2 Hz, 2H), 1.84 (m, 2H), 1.72 (m, 2H), 1.55 (m, 2H); ^{13}C NMR (100 MHz, $CDCl_3$) δ (ppm): 159.0, 145.2, 141.2, 137.3, 132.6, 132.5, 128.5, 128.1, 127.6, 127.5, 127.3, 119.7, 119.0, 114.9, 110.8, 67.7, 29.0, 28.4, 25.4, 25.4, 17.1. IR (cm^{-1}): 2933, 2861, 2251, 2227, 1600, 1490, 1468, 1252, 811. GC-MS: No peak
DSC: K 133 Sm 160 N 248 I 247 N 154 Sm 105 K

POM: K 146 Sm 158 N 244.7 I 244.6 N 154 Sm 105 K

SI.2 Synthesis of PF6OCB

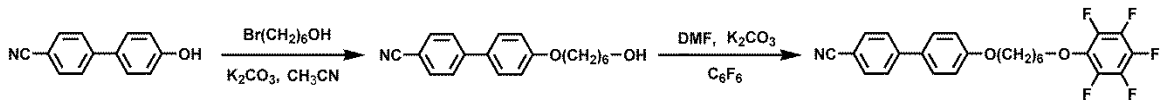

4'-[(6-hydroxyhexyl)oxy]-4-cyanobiphenyl. To a stirred solution of 4'-hydroxy-4-cyanobiphenyl (0.8 g, 4.6 mmol) in acetonitrile (35 mL) was added potassium carbonate (1.3 g, 9.2 mmol) and the mixture was kept under reflux for half an hour. Then 6-bromohexanol (1.0 g, 5.52 mmol) was added and the reaction was stirred overnight under reflux. After cooling, the solvent was removed under reduced pressure and the product was extracted with dichloromethane (50 mL), washed with water (150 mL), dried over magnesium sulfate filtered and evaporated. The crude product was subjected to flash column chromatography on silica gel (ethyl acetate and hexane 15%: 85%) to afford the desired product; (1.02 g, 75%).

^{1}H NMR (400 MHz, $CDCl_3$) δ (ppm): 7.68 (d, *J* = 8.68 Hz, 2H), 7.63 (d, *J* = 8.68 Hz, 2H), 7.52 (d, *J* = 8.88 Hz, 2H), 6.98 (d, J = 8.78 Hz, 2H), 4.01 (t, *J* = 6.49 Hz, 2H), 3.69-3.65 (m, 2H), 1.85-1.81 (m, 2H), 1.64-1.60 (m, 2H), 1.52-1.45 (m, 4H); ^{13}C NMR (100 MHz, $CDCl_3$) δ (ppm): 159.75, 145.28, 132.58, 131.31, 128.32, 127.09, 119.15, 115.08, 110.03, 68.01, 62.89, 32.67, 29.20, 25.90, 25.56.

PF6OCB. In a 200 ml round bottom flask was placed 4'-[(6-hydroxyhexyl)oxy]-4-cyanobiphenyl (2.95 g, 10.0 mmol), hexafluorobenzene (3.72 g, 20.0 mmol. 2.0 equiv.), dry DMF (15.0 ml), potassium carbonate (1.38 g, 10.0 mmol, 1.0 equiv.) and potassium iodide (0.1 equiv.). The resulting suspension was stirred at 40-50 °C overnight and the reaction was monitored by TLC analysis. Upon completion, water was added dropwise with stirring to fill the flask and then the mixture was extracted with ethyl acetate. The organic layers were washed with water and dried over $MgSO_4$. The product was purified by flash chromatography as a low melting white solid. (2.6 g, 57%)

^{1}H NMR (400 MHz, $CDCl_3$) δ (ppm): 7.70 (m, 2H), 7.64 (m, 2H), 7.53 (dd, ^{1}J = 6.8 Hz, ^{2}J = 2.8 Hz, 2H), 6.99 (td, ^{1}J = 8.8 Hz, ^{2}J = 3.2 Hz, 2H), 4.17 (t, J = 6.4 Hz, 2H), 4.03 (t, J = 6.4 Hz, 2H), 1.87-1.80 (m, 4H), 1.58-1.55 (m, 4H); ^{13}C NMR (100 MHz, $CDCl_3$) δ (ppm): 159.7, 145.3, 132.6, 131.4, 128.4, 127.1, 119.1, 115.1, 110.1, 75.6, 67.9, 29.8, 29.1, 25.7, 25.3; ^{19}F NMR (376 MHz, $CDCl_3$) δ (ppm): -156.93 (m, 2F), -163.43 (m, 2F), -163.67 (m, 1F).

Cl5OCB (General Procedure A)

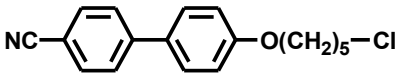

White crystals recrystallized from methanol. (890 mg, yield: 60%)

^{1}H NMR (400 MHz, $CDCl_3$) δ (ppm): 7.70 (m, 2H), 7.64 (m, 2H), 7.53 (td, ^{1}J = 8.8 Hz, ^{2}J = 2.8 Hz, 2H), 6.99 (td, ^{1}J = 8.8 Hz, ^{2}J = 2.8 Hz, 2H), 4.03 (t, J = 5.6 Hz, 2H), 3.58 (t, J = 6.8 Hz, 2H), 1.91-1.82 (m, 4H), 1.65 (m, 2H); ^{13}C NMR (100 MHz, $CDCl_3$) δ (ppm): 159.3, 145.2, 132.6, 131.4, 128.4, 127.1, 119.1, 115.1, 110.1, 67.8, 44.9, 32.3, 28.5, 23.5. GC-MS:299.18 found 299.79 calc.

SI. 3 The NMR spectra of representative compounds

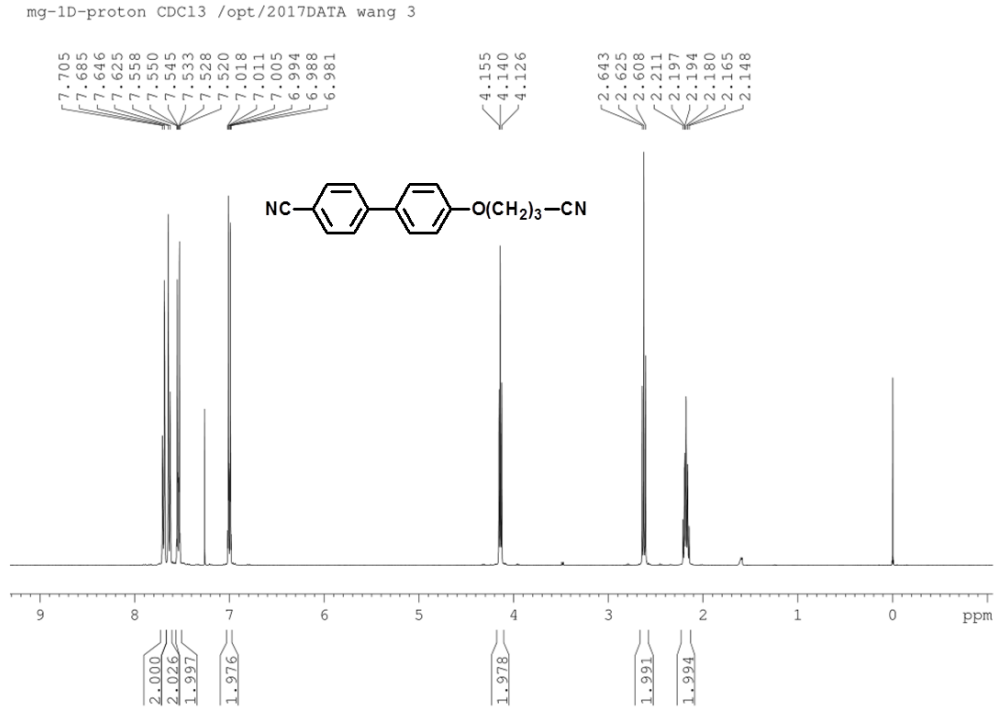

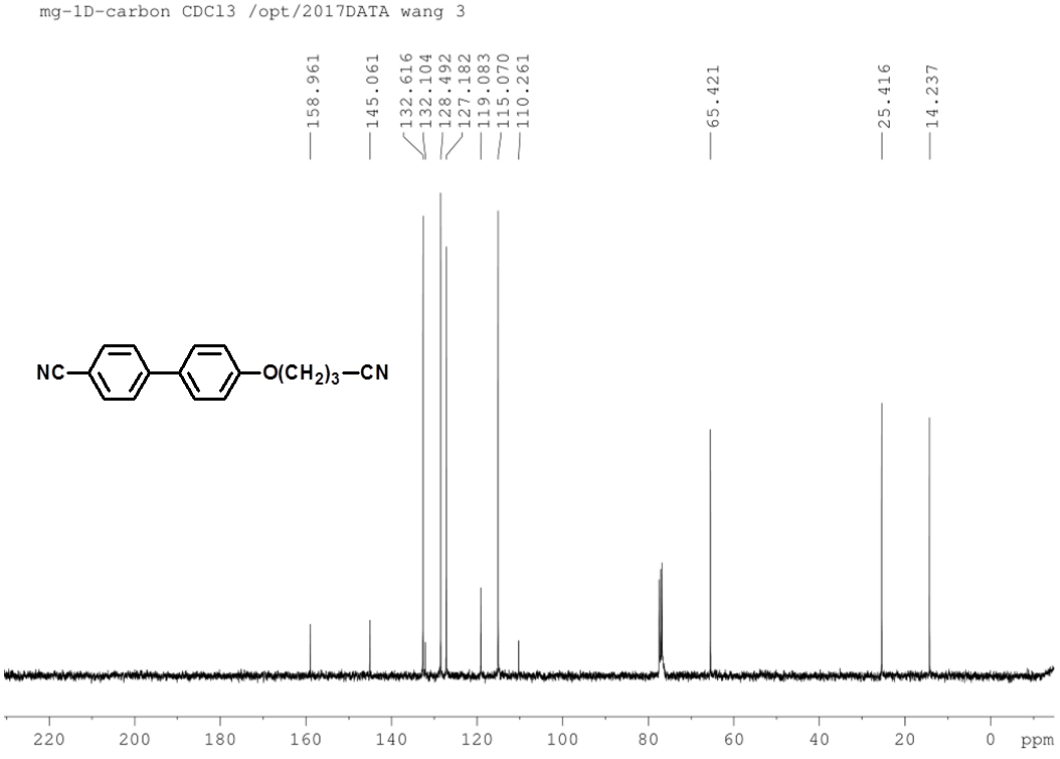

mg-1D-proton CDCl3 /opt/2017DATA wang 9

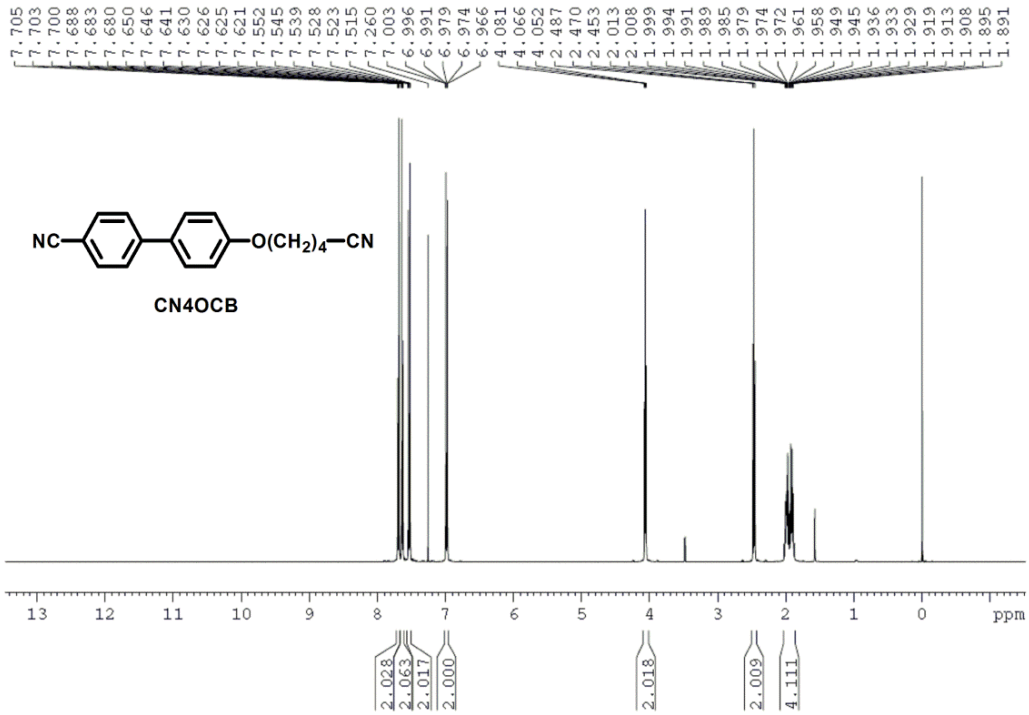

mg-1D-carbon CDCl3 /opt/2017DATA wang 4

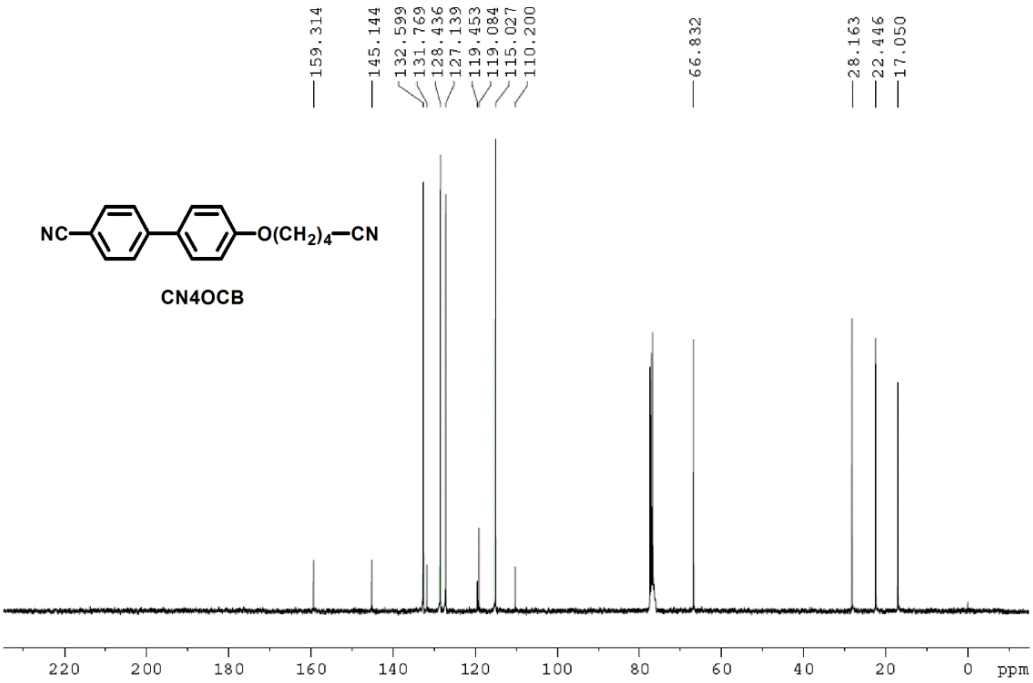

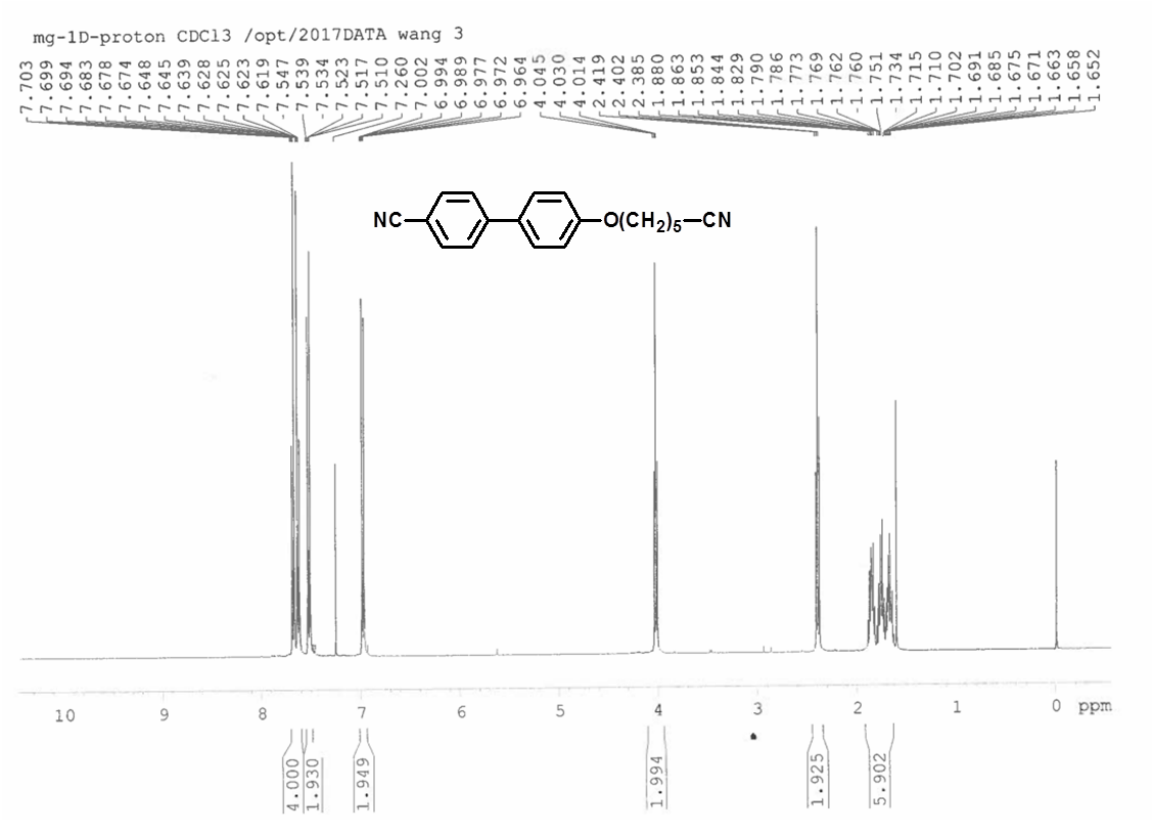
mg-1D-proton CDCl3 /opt/2017DATA wang 3
7.703
7.699
7.694
7.683
7.678
7.674
7.648
7.645
7.639
7.628
7.625
7.623
7.619
7.547
7.539
7.534
7.523
7.517
7.510
7.260
7.002
6.994
6.989
6.977
6.972
6.964
4.045
4.030
4.014
2.419
2.402
2.385
1.880
1.863
1.853
1.844
1.829
1.790
1.786
1.773
1.769
1.762
1.760
1.751
1.734
1.715
1.710
1.702
1.691
1.685
1.675
1.671
1.663
1.658
1.652
NC
O(CH2)5—CN
10
9
8
7
6
5
4
3
2
1
0
ppm
4.000
1.930
1.949
1.994
1.925
5.902

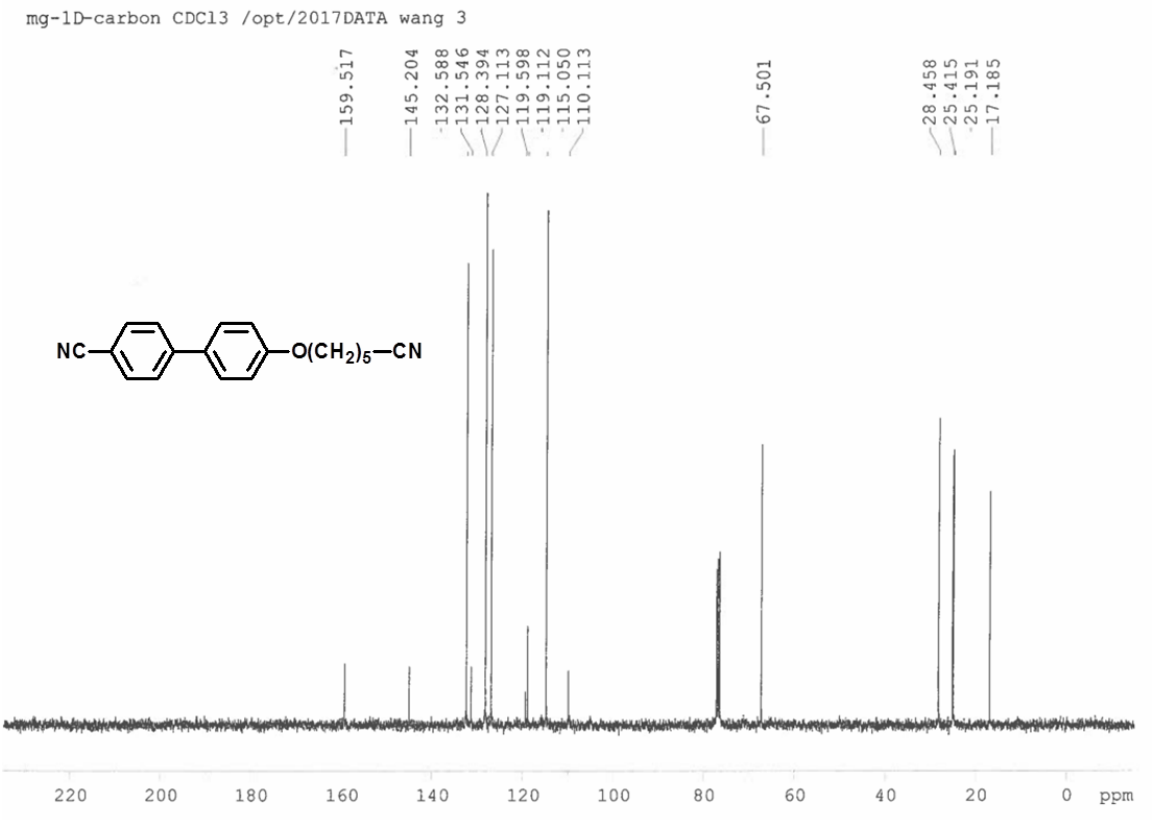
mg-1D-carbon CDCl3 /opt/2017DATA wang 3
159.517
145.204
132.588
131.546
128.394
127.113
119.598
119.112
115.050
110.113
67.501
28.458
25.415
25.191
17.185
NC
O(CH2)5—CN
220
200
180
160
140
120
100
80
60
40
20
0
ppm

mg-1D-proton CDCl3 /opt/2017DATA wang 10

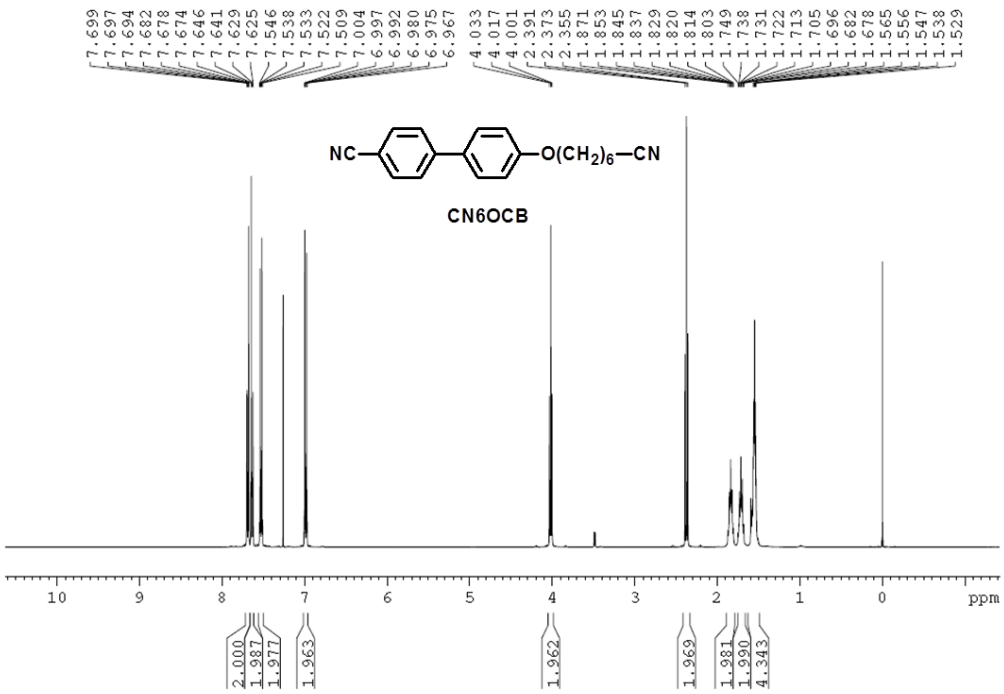

mg-1D-carbon CDCl3 /opt/2017DATA wang 5

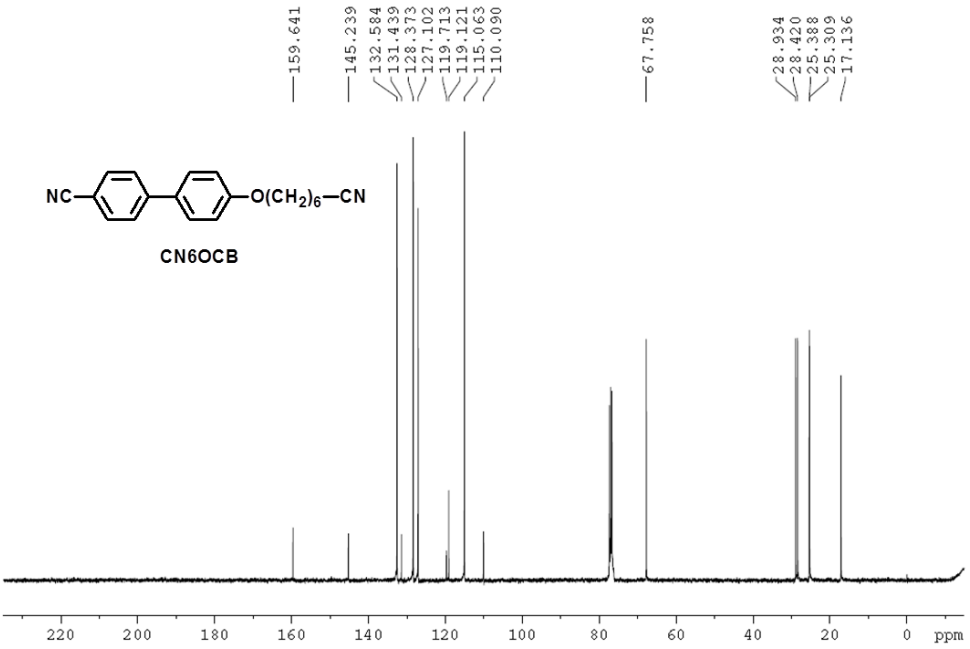

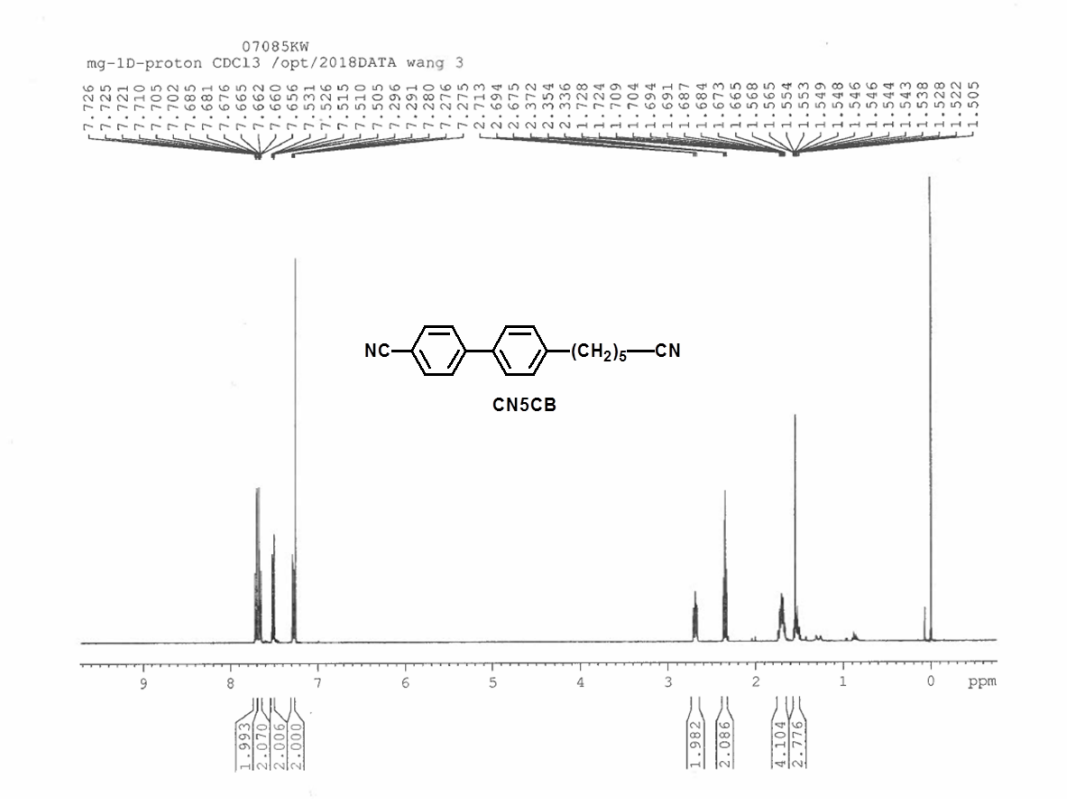
07085KW
mg-1D-proton CDCl3 /opt/2018DATA wang 3
7.726 7.725 7.721 7.710 7.705 7.702 7.685 7.681 7.676 7.665 7.662 7.660 7.656 7.531 7.526 7.515 7.510 7.505 7.296 7.291 7.280 7.276 7.275 2.713 2.694 2.675 2.372 2.354 2.336 1.728 1.724 1.709 1.704 1.694 1.691 1.687 1.684 1.673 1.665 1.568 1.565 1.554 1.553 1.549 1.548 1.546 1.546 1.544 1.543 1.538 1.528 1.522 1.505
NC
(CH2)5
CN
CN5CB
9 8 7 6 5 4 3 2 1 0 ppm
1.993 2.070 2.006 2.000 1.982 2.086 4.104 2.776

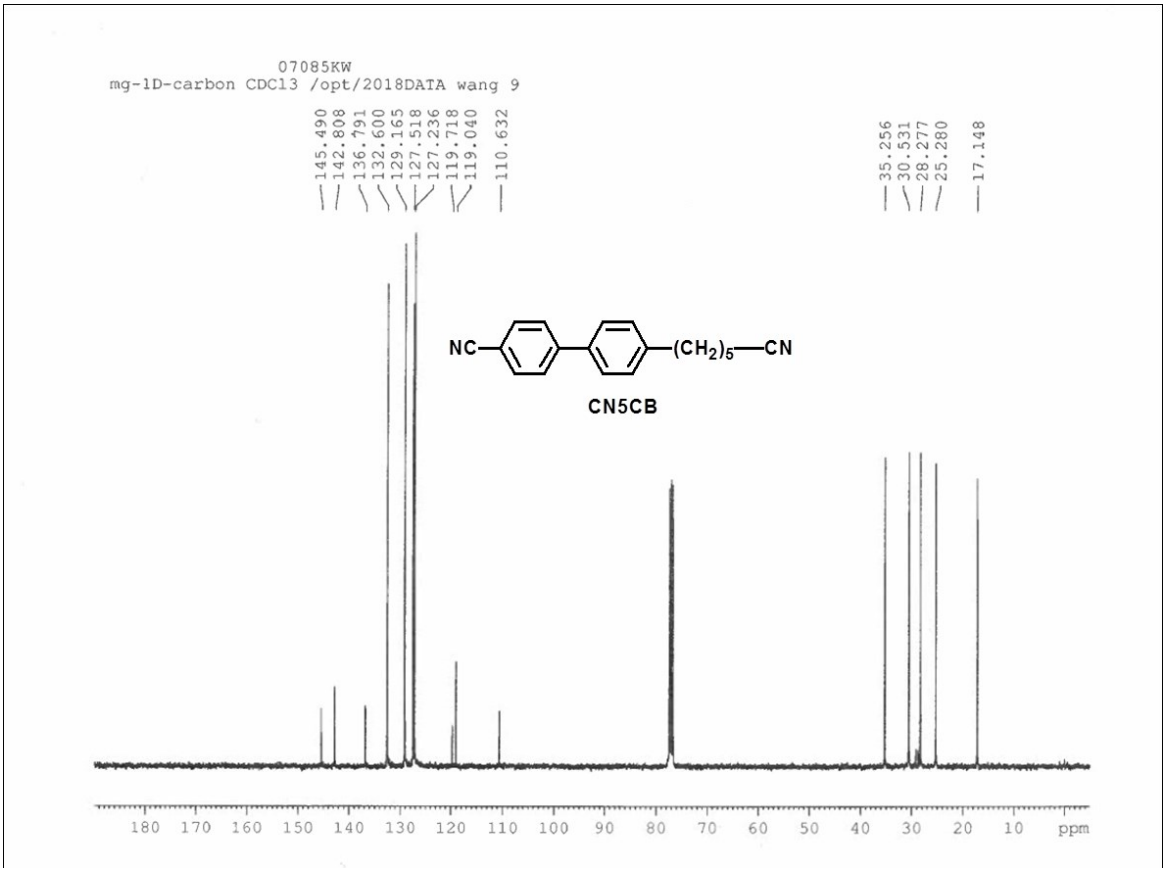
07085KW
mg-1D-carbon CDCl3 /opt/2018DATA wang 9
145.490 142.808 136.791 132.600 129.165 127.518 127.236 119.718 119.040 110.632
35.256 30.531 28.277 25.280 17.148
NC
(CH2)5
CN
CN5CB
180 170 160 150 140 130 120 110 100 90 80 70 60 50 40 30 20 10 ppm

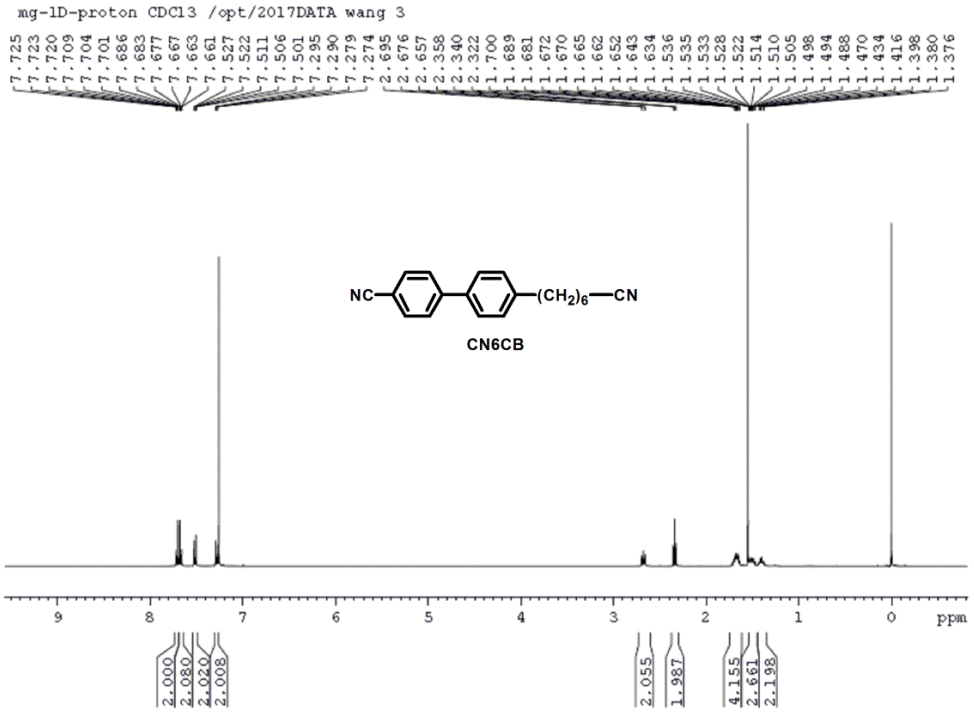
mg-1D-proton CDCl3 /opt/2017DATA wang 3
7.725
7.723
7.720
7.709
7.704
7.701
7.686
7.683
7.677
7.667
7.663
7.661
7.527
7.522
7.511
7.506
7.501
7.295
7.290
7.279
7.274
2.695
2.676
2.657
2.358
2.340
2.322
1.700
1.689
1.681
1.672
1.670
1.665
1.662
1.652
1.643
1.634
1.536
1.535
1.533
1.528
1.522
1.514
1.510
1.505
1.498
1.494
1.488
1.470
1.434
1.416
1.398
1.380
1.376
NC
(CH2)6
CN
CN6CB
9
8
7
6
5
4
3
2
1
0
ppm
2.000
2.080
4.020
2.008
2.055
1.987
4.155
2.661
2.198

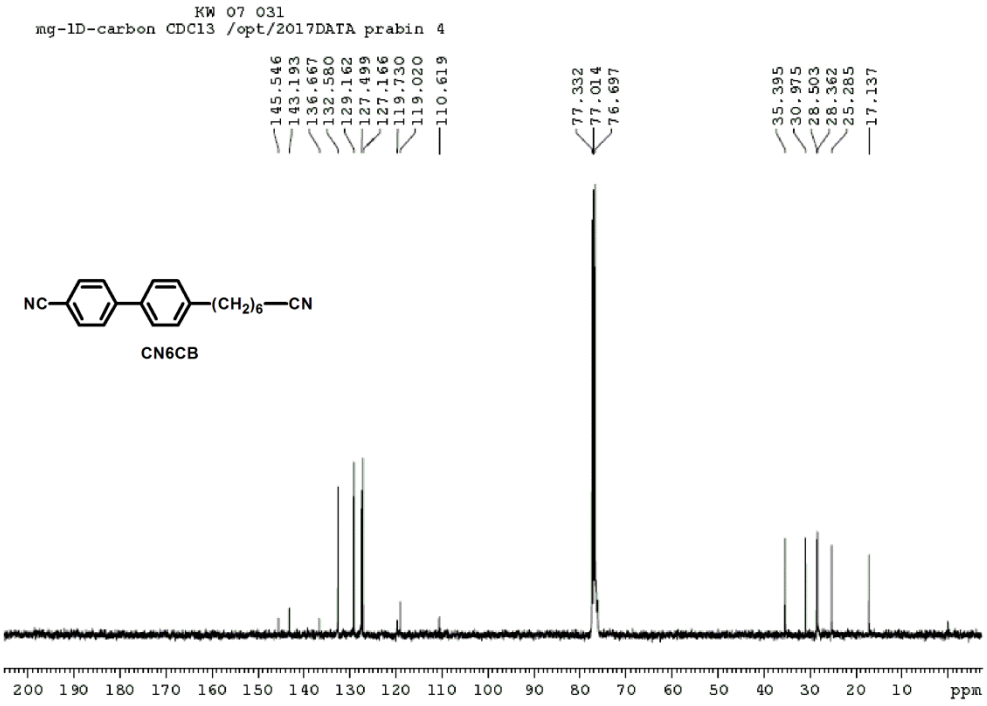
KW 07 031
mg-1D-carbon CDCl3 /opt/2017DATA prabin 4
145.546
143.193
136.667
132.580
129.162
127.499
127.166
119.730
119.020
110.619
77.332
77.014
76.697
35.395
30.975
28.503
28.362
25.285
17.137
NC
(CH2)6
CN
CN6CB
200
190
180
170
160
150
140
130
120
110
100
90
80
70
60
50
40
30
20
10
ppm

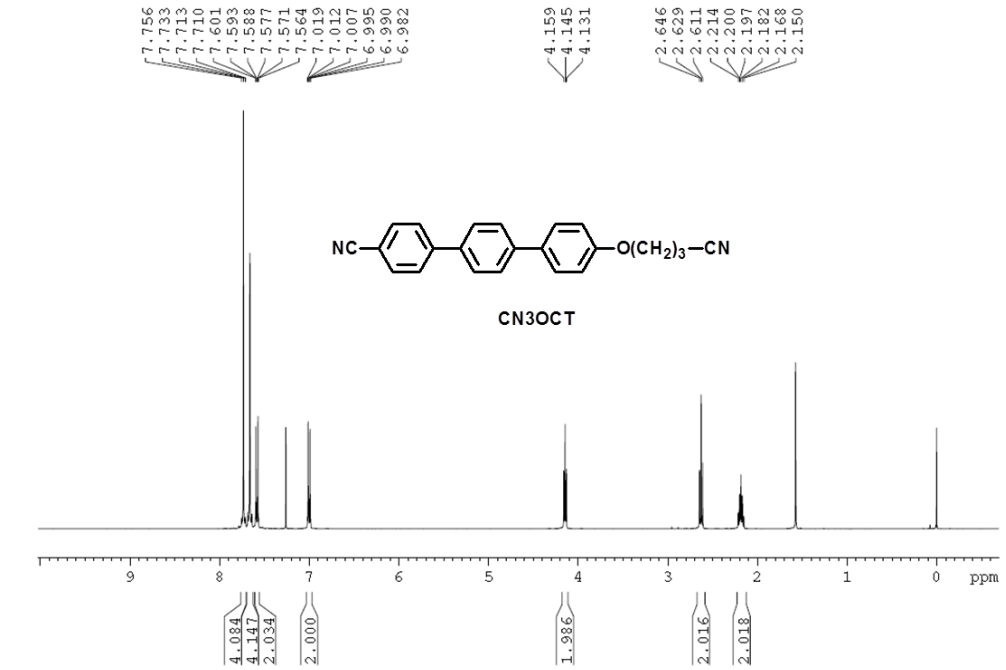
7.756
7.733
7.713
7.710
7.601
7.593
7.588
7.577
7.571
7.564
7.019
7.012
7.007
6.995
6.990
6.982
4.159
4.145
4.131
2.646
2.629
2.611
2.214
2.200
2.197
2.182
2.168
2.150
NC
O(CH2)3—CN
CN3OCT
9
8
7
6
5
4
3
2
1
0
ppm
4.084
4.147
2.034
2.000
1.986
2.016
2.018

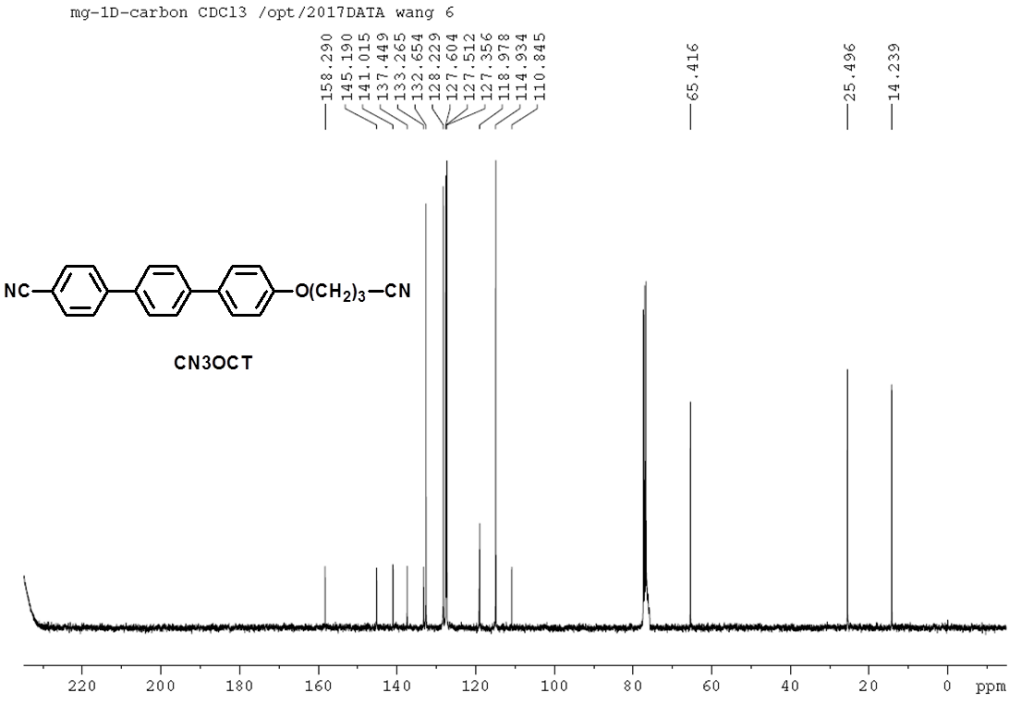
mg-1D-carbon CDCl3 /opt/2017DATA wang 6
158.290
145.190
141.015
137.449
133.265
132.654
128.229
127.604
127.512
127.356
118.978
114.934
110.845
65.416
25.496
14.239
NC
O(CH2)3—CN
CN3OCT
220
200
180
160
140
120
100
80
60
40
20
0
ppm

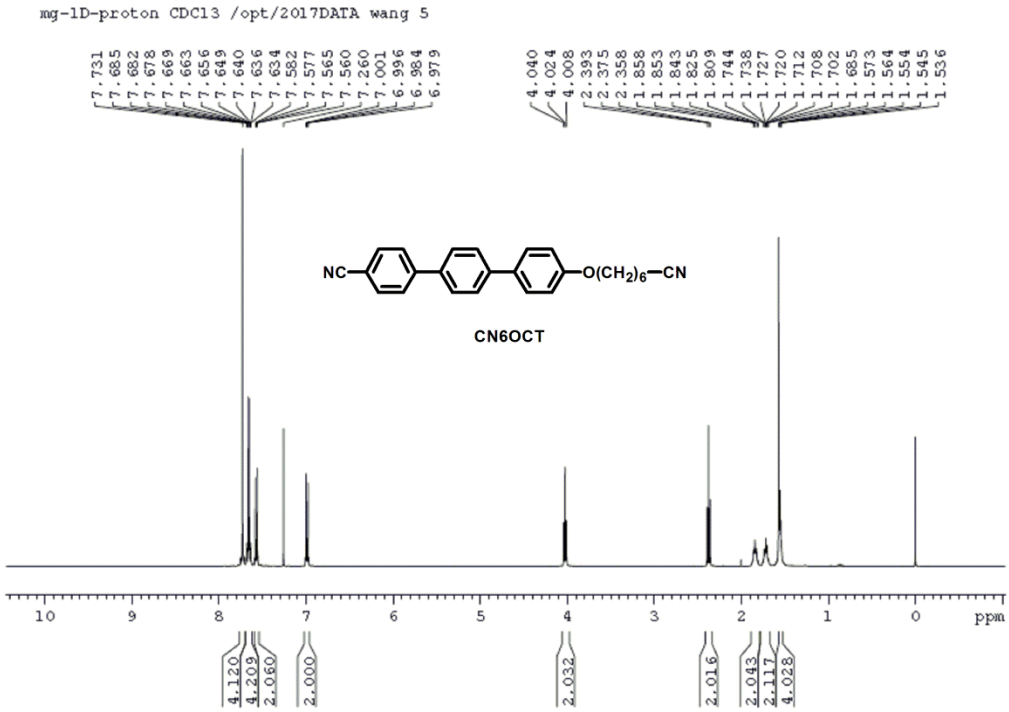
mg-1D-proton CDCl3 /opt/2017DATA wang 5
7.731
7.685
7.682
7.678
7.669
7.663
7.656
7.649
7.640
7.636
7.634
7.582
7.577
7.565
7.560
7.260
7.001
6.996
6.984
6.979
4.040
4.024
4.008
2.393
2.375
2.358
1.858
1.853
1.843
1.825
1.809
1.744
1.738
1.727
1.720
1.712
1.708
1.702
1.685
1.573
1.564
1.554
1.545
1.536
NC
O(CH2)6—CN
CN6OCT
10
9
8
7
6
5
4
3
2
1
0
ppm
4.120
4.209
2.060
2.000
2.032
2.016
2.043
2.117
4.028

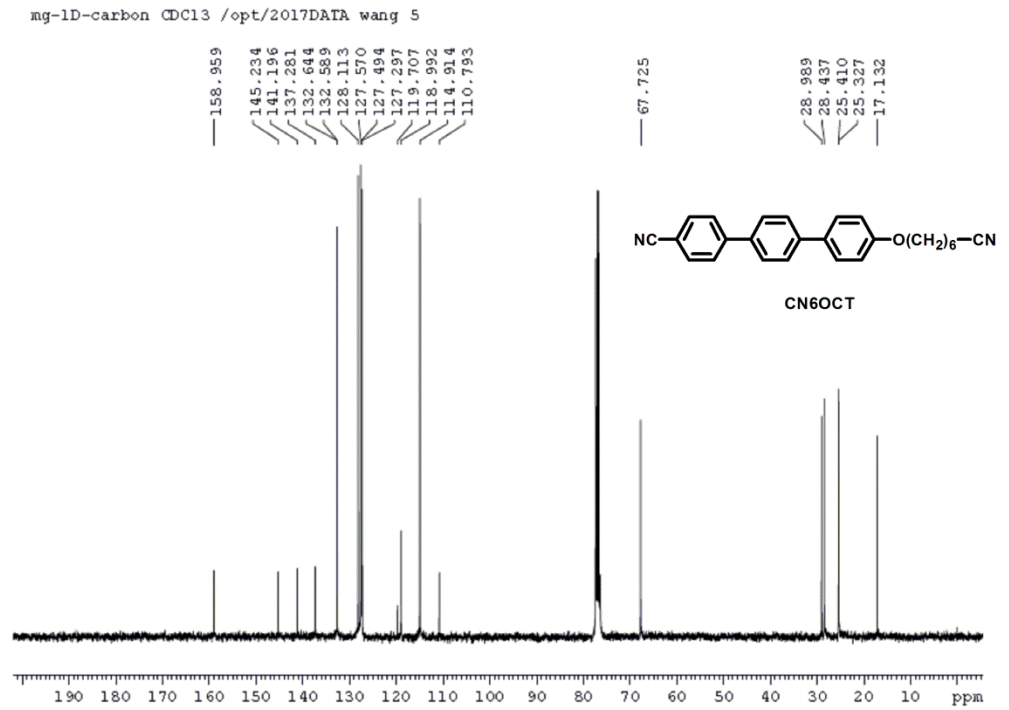
mg-1D-carbon CDCl3 /opt/2017DATA wang 5
158.959
145.234
141.196
137.281
132.644
132.589
128.113
127.570
127.494
127.297
119.707
118.992
114.914
110.793
67.725
28.989
28.437
25.410
25.327
17.132
NC
O(CH2)6—CN
CN6OCT
190
180
170
160
150
140
130
120
110
100
90
80
70
60
50
40
30
20
10
ppm

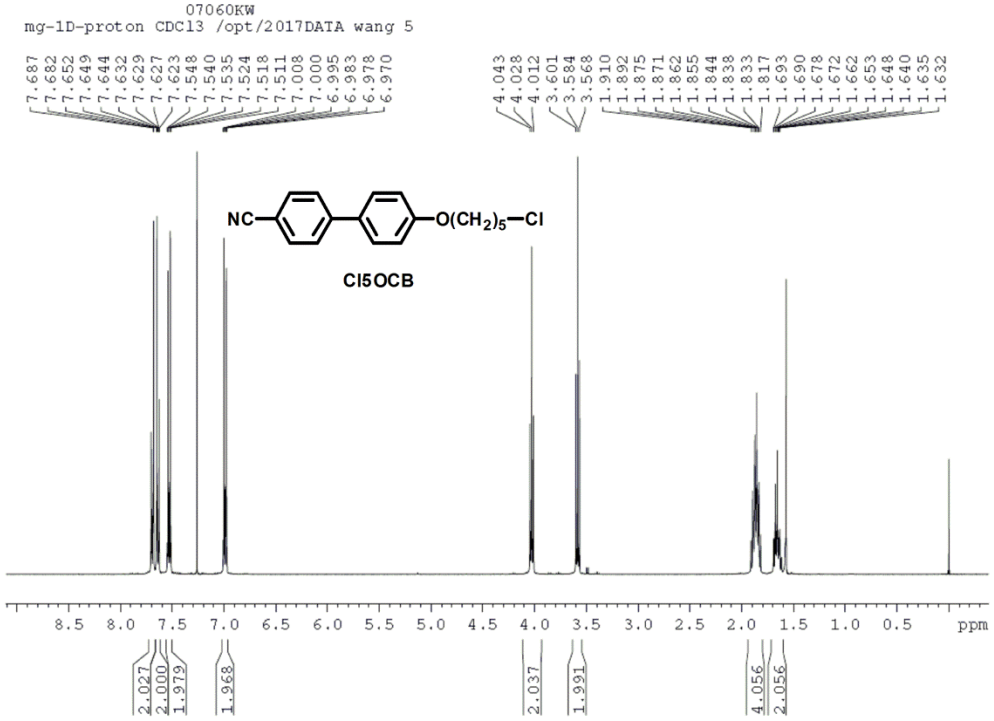
07060KW
mg-1D-proton CDCl3 /opt/2017DATA wang 5
7.687
7.682
7.652
7.649
7.644
7.632
7.629
7.627
7.623
7.548
7.540
7.535
7.524
7.518
7.511
7.008
7.000
6.995
6.983
6.978
6.970
4.043
4.028
4.012
3.601
3.584
3.568
1.910
1.892
1.875
1.871
1.862
1.855
1.844
1.838
1.833
1.817
1.693
1.690
1.678
1.672
1.662
1.653
1.648
1.640
1.635
1.632
NC
O(CH2)5—Cl
Cl5OCB
8.5 8.0 7.5 7.0 6.5 6.0 5.5 5.0 4.5 4.0 3.5 3.0 2.5 2.0 1.5 1.0 0.5 ppm
2.027
2.000
1.979
1.968
2.037
1.991
4.056
2.056

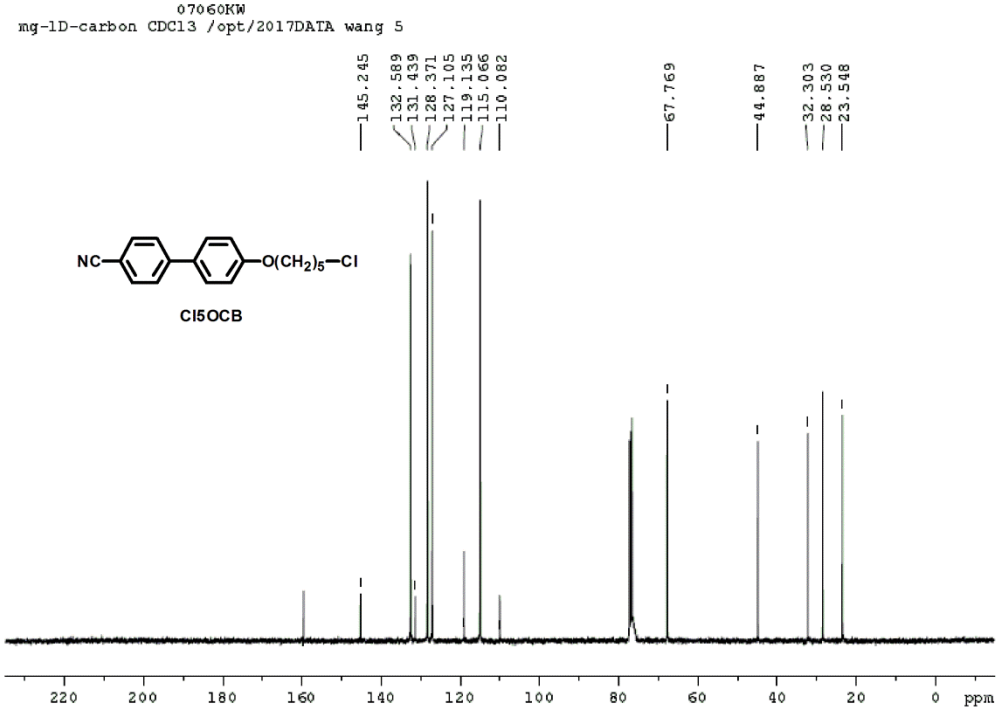
07060KW
mg-1D-carbon CDCl3 /opt/2017DATA wang 5
145.245
132.589
131.439
128.371
127.105
119.135
115.066
110.082
67.769
44.887
32.303
28.530
23.548
NC
O(CH2)5—Cl
Cl5OCB
220 200 180 160 140 120 100 80 60 40 20 0 ppm

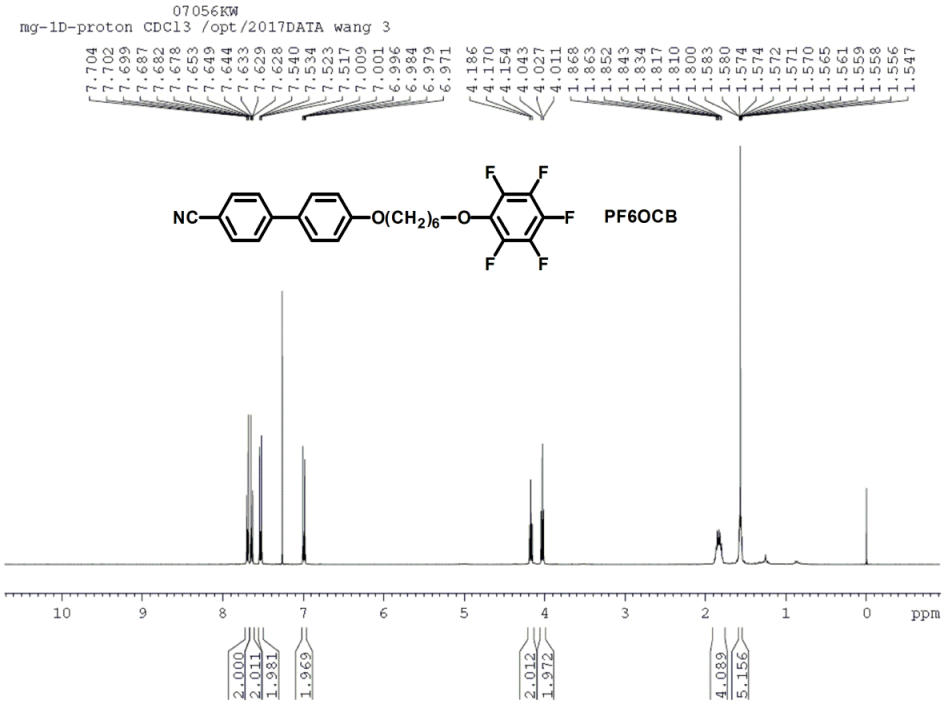
07056KW
mg-1D-proton CDCl3 /opt/2017DATA wang 3
7.704
7.702
7.699
7.687
7.682
7.678
7.653
7.649
7.644
7.633
7.629
7.628
7.540
7.534
7.523
7.517
7.009
7.001
6.996
6.984
6.979
6.971
4.186
4.170
4.154
4.043
4.027
4.011
1.868
1.863
1.852
1.843
1.834
1.817
1.810
1.800
1.583
1.580
1.574
1.574
1.572
1.571
1.570
1.565
1.561
1.559
1.558
1.556
1.547
NC
O(CH2)6
O
F
PF6OCB
10
9
8
7
6
5
4
3
2
1
0
ppm
2.000
2.011
1.981
1.969
2.012
1.972
4.089
5.156

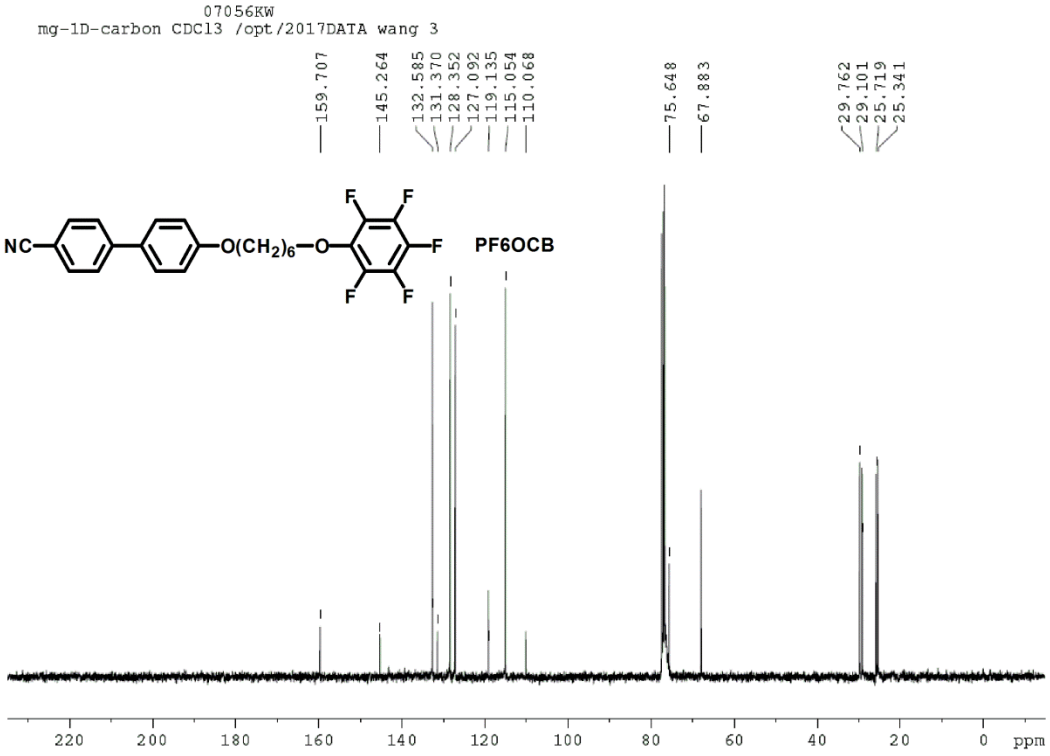
07056KW
mg-1D-carbon CDCl3 /opt/2017DATA wang 3
159.707
145.264
132.585
131.370
128.352
127.092
119.135
115.054
110.068
75.648
67.883
29.762
29.101
25.719
25.341
NC
O(CH2)6
O
F
PF6OCB
220
200
180
160
140
120
100
80
60
40
20
0
ppm

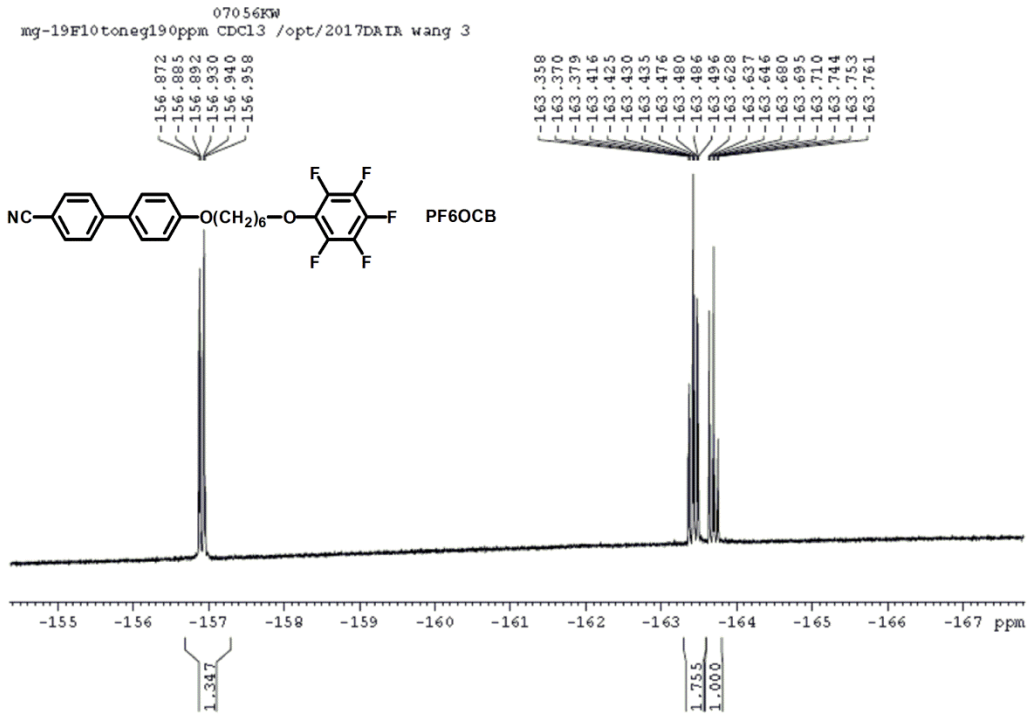
07056KW
mg-19F10toneg190ppm CDCl3 /opt/2017DATA wang 3
-156.872
-156.885
-156.892
-156.930
-156.940
-156.958
-163.358
-163.370
-163.379
-163.416
-163.425
-163.430
-163.435
-163.476
-163.480
-163.486
-163.496
-163.628
-163.637
-163.646
-163.680
-163.695
-163.710
-163.744
-163.753
-163.761
NC
O(CH2)6
O
F
PF6OCB
-155
-156
-157
-158
-159
-160
-161
-162
-163
-164
-165
-166
-167 ppm
1.347
1.755
1.000

SI. 4 The DSC plots of the cyano tail terminated liquid crystals that are not shown in the main text. (The second heating cooling cycle is shown for all cases)

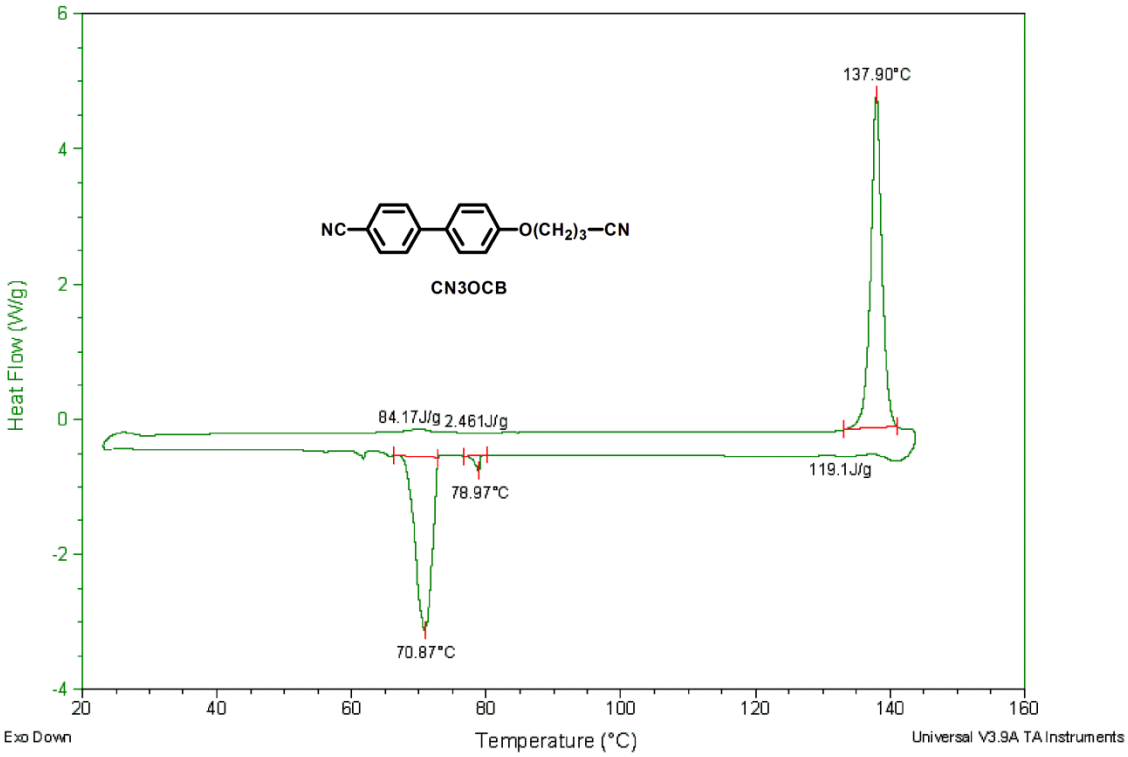

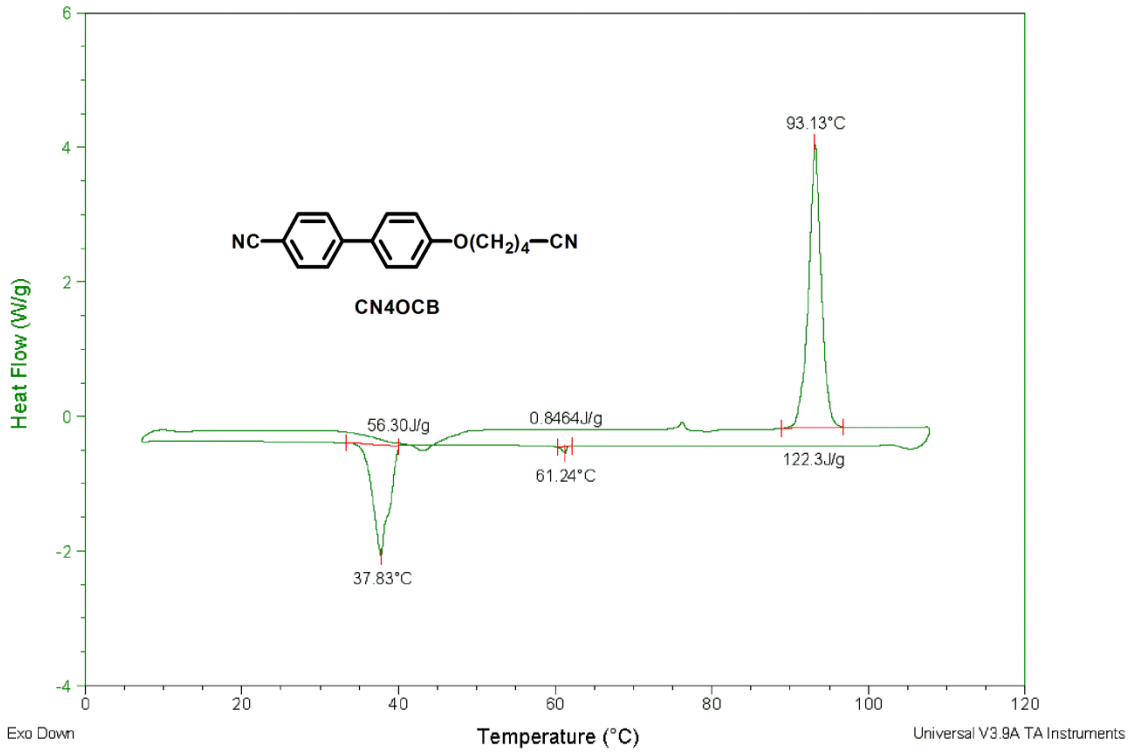

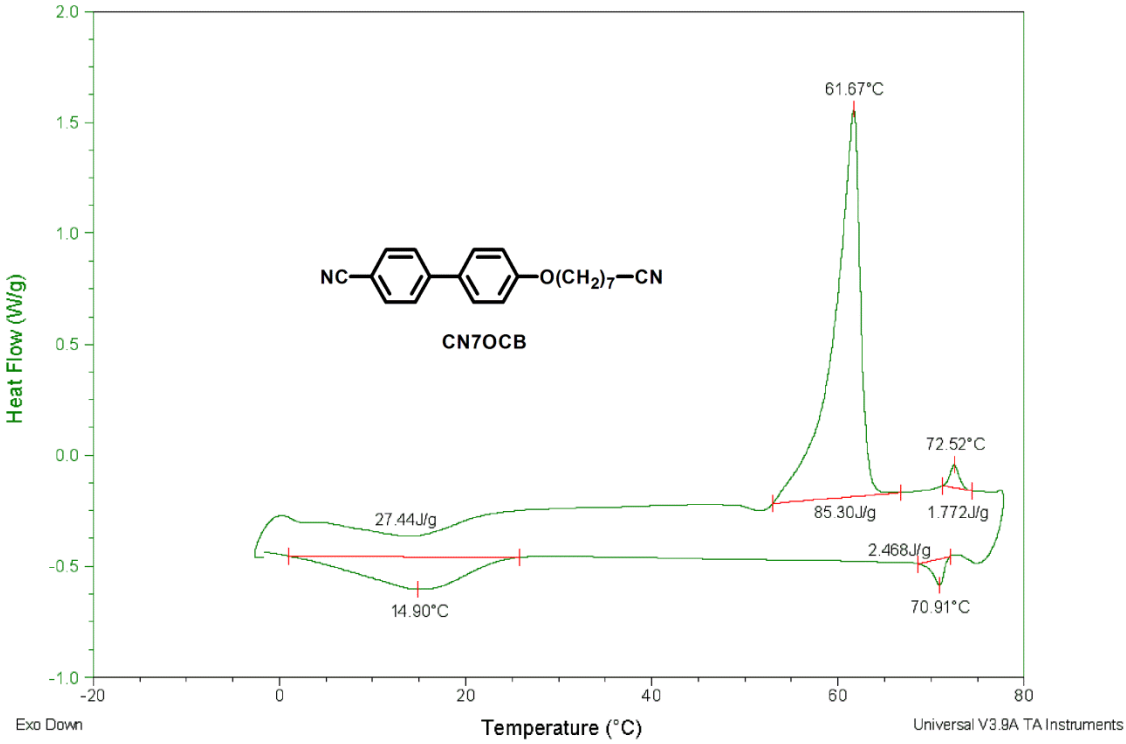
Heat Flow (W/g)
2.0
1.5
1.0
0.5
0.0
-0.5
-1.0
NC
O(CH2)7CN
CN7OCB
61.67°C
72.52°C
27.44J/g
85.30J/g
1.772J/g
2.468J/g
14.90°C
70.91°C
-20
0
20
40
60
80
Exo Down
Temperature (°C)
Universal V3.9A TA Instruments

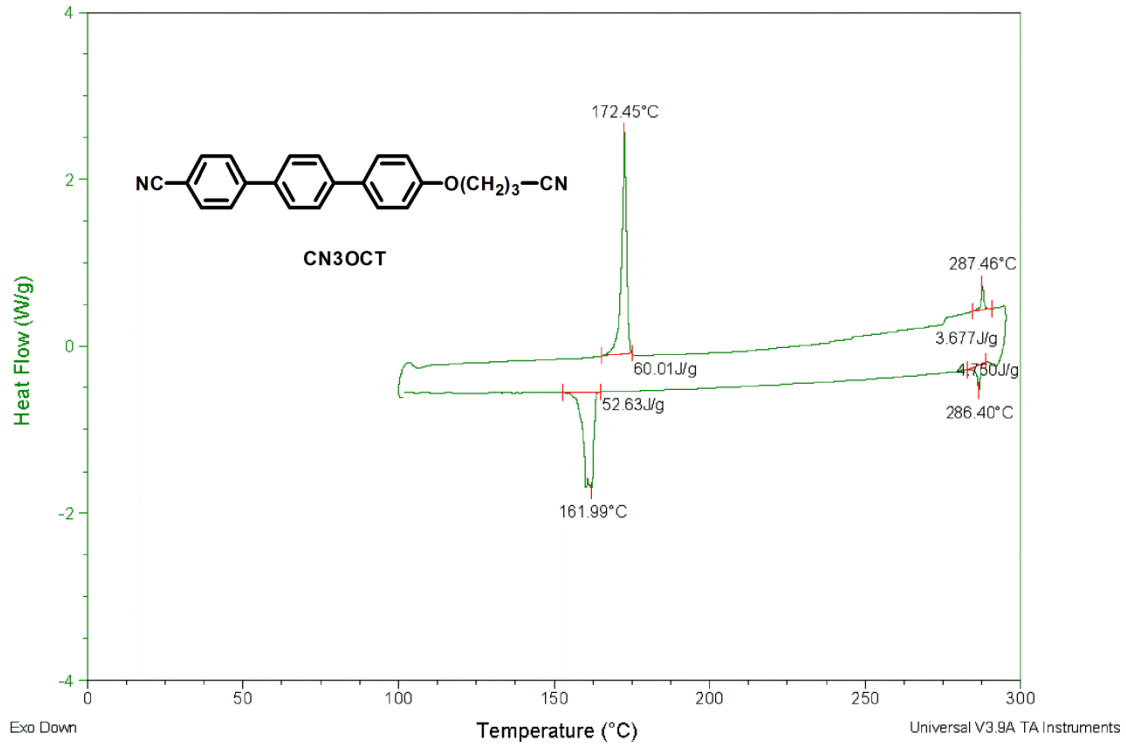
Heat Flow (W/g)
4
2
0
-2
-4
NC
O(CH2)3CN
CN3OCT
172.45°C
287.46°C
3.677J/g
60.01J/g
52.63J/g
286.40°C
161.99°C
0
50
100
150
200
250
300
Exo Down
Temperature (°C)
Universal V3.9A TA Instruments

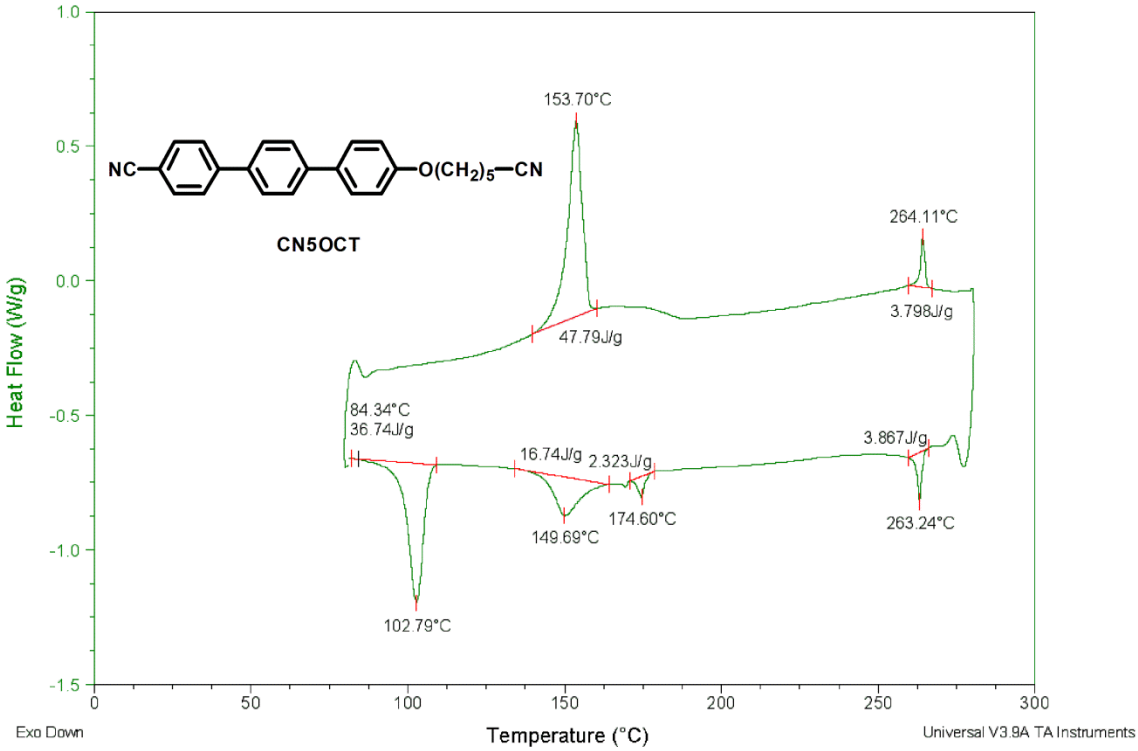
NC
O(CH2)5CN
CN5OCT
153.70°C
264.11°C
47.79J/g
3.798J/g
84.34°C
36.74J/g
16.74J/g
2.323J/g
3.867J/g
174.60°C
149.69°C
263.24°C
102.79°C
Heat Flow (W/g)
Temperature (°C)
Exo Down
Universal V3.9A TA Instruments

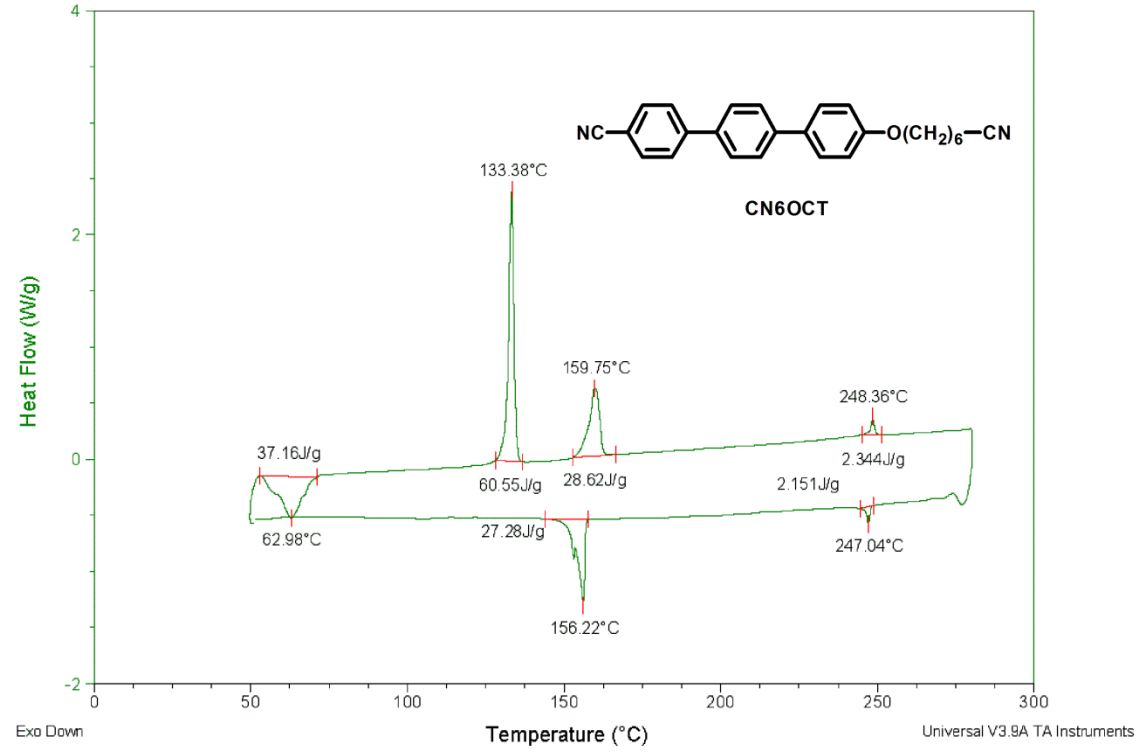
NC
O(CH2)6CN
CN6OCT
133.38°C
159.75°C
248.36°C
37.16J/g
60.55J/g
28.62J/g
2.344J/g
2.151J/g
62.98°C
27.28J/g
247.04°C
156.22°C
Heat Flow (W/g)
Temperature (°C)
Exo Down
Universal V3.9A TA Instruments

SI.5. Dipole moment and Gibbs Free Energy of adsorption for cyano-terminated compounds

Table SI.1. Calculated dipole moment of the 4'-ω-cyanoalkyl-4-cyanobiphenyl, 4'-ω-cyanoalkoxy-4-cyanobiphenyl, and 4'-ω-cyanoalkoxy-4-cyanoterphenyl compounds. 'n' indicates the number of CH_2 groups defined by the molecular formula in each column.

n	NC–C6H4–C6H4–(CH2)n–CN	NC–C6H4–C6H4–O(CH2)n–CN	NC–C6H4–C6H4–C6H4–O(CH2)n–CN
2	8.07	8.38	8.42
3	8.35	8.39	8.43
4	8.48	8.79	8.91
5	8.63	8.81	8.93
6	8.71	9.23	9.49
7	9.01	9.72	9.82

Table SI.2. Calculated Gibbs Free Energy of adsorption (G_{BE}; in eV) for the 4'-ω-cyanoalkyl-4-cyanobiphenyl, 4'-ω-cyanoalkoxy-4-cyanobiphenyl, and 4'-ω-cyanoalkoxy-4-cyanoterphenyl compounds onto $Al(ClO_4)_3$, $Ga(ClO_4)_3$, and $Ni(ClO_4)_2$. Here 'n' indicates the number of CH_2 groups defined by the molecular formula in each column. 'Ph' and 'CH_2' refer to the neighboring group of the coordinating CN, thus identifying which CN end of the compound binds to the metal cation.

n	NC–C6H4–C6H4–(CH2)n–CN						NC–C6H4–C6H4–O(CH2)n–CN						NC–C6H4–C6H4–C6H4–O(CH2)n–CN					
	$Al(ClO_4)_3$		$Ga(ClO_4)_3$		$Ni(ClO_4)_2$		$Al(ClO_4)_3$		$Ga(ClO_4)_3$		$Ni(ClO_4)_2$		$Al(ClO_4)_3$		$Ga(ClO_4)_3$		$Ni(ClO_4)_2$	
	Ph	CH_2	Ph	CH_2	Ph	CH_2	Ph	CH_2	Ph	CH_2	Ph	CH_2	Ph	CH_2	Ph	CH_2	Ph	CH_2
2	-0.45	-0.45	-0.56	-0.56	-1.06	-1.04	-0.46	-0.24	-0.56	-0.35	-1.07	-1.00	-0.44	-0.31	-0.56	-0.41	-1.06	-1.00
3	-0.45	-0.45	-0.55	-0.54	-1.06	-1.05	-0.46	-0.36	-0.55	-0.45	-1.07	-1.02	-0.45	-0.38	-0.56	-0.46	-1.05	-1.00
4	-0.45	-0.44	-0.56	-0.56	-1.07	-1.06	-0.45	-0.41	-0.56	-0.50	-1.07	-1.08	-0.45	-0.39	-0.55	-0.52	-1.06	-1.04
5	-0.45	-0.44	-0.57	-0.57	-1.06	-1.05	-0.45	-0.41	-0.57	-0.51	-1.08	-1.07	-0.45	-0.40	-0.57	-0.53	-1.05	-1.05
6	-0.46	-0.44	-0.56	-0.56	-1.06	-1.04	-0.46	-0.41	-0.55	-0.54	-1.08	-1.07	-0.45	-0.40	-0.55	-0.55	-1.05	-1.04
7	-0.46	-0.44	-0.57	-0.56	-1.06	-1.06	-0.45	-0.41	-0.55	-0.54	-1.07	-1.07	-0.44	-0.40	-0.56	-0.56	-1.05	-1.04

SI.6. Anchoring Study of the Binary Mixtures of PF6OCB and Cl5OCB in 50%:50% Molar Ratio on $Ni(ClO_4)_2$-Coated Surfaces and Air Free Interface

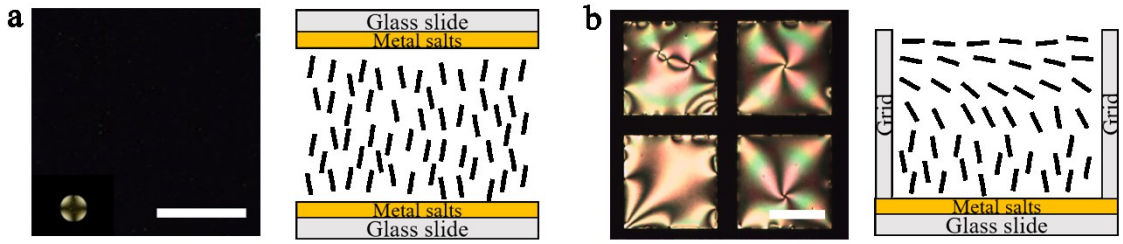

[1] Chen L, Chen Y, Zhou W, et al. Synthesis and properties of light-emitting polythiophene derivatives bearing terphenyl mesogenic pendant, Mol Cryst Liq Cryst. 2010; 518(1): 70–83.